Eur. Phys. J. Spec. Top. (2022) 231:3–26
https://doi.org/10.1140/epjs/s11734-021-00396-3

THE EUROPEAN PHYSICAL JOURNAL SPECIAL TOPICS

Review

Ground-based gamma-ray astronomy: history and development of techniques

D. Bose[1,a], V. R. Chitnis[2], P. Majumdar[3,4], and B. S.Acharya[2]

[1] Department of Astrophysics and Cosmology, S. N. Bose National Centre for Basic Sciences, Kolkata, India
[2] Department of High Energy Physics, Tata Institute of Fundamental Research, Mumbai, India
[3] High Energy Nuclear and Particle Physics Division, Saha Institute of Nuclear Physics, Kolkata, India
[4] Department of Astrophysics, Faculty of Physics and Applied Informatics, University of Lodz, Lodz, Poland

Received 1 November 2021 / Accepted 13 December 2021 / Published online 30 December 2021

Abstract Very high energy (VHE) γ-rays constitute one of the main pillars of high energy astrophysics. Gamma-rays are produced under extreme relativistic conditions in the Universe. VHE γ-rays can be detected indirectly on the ground. Detection of these energetic photons poses several technological challenges. First, even though γ-rays are highly penetrative, the Earth's atmosphere is opaque to them. Second, these γ-rays are to be detected against the overwhelming background of cosmic rays. When a VHE γ-ray arrives at the top of the atmosphere, it produces charged secondaries. These charged particles produce Cherenkov flashes in optical band. Even though first attempts to detect these Cherenkov flashes were made almost 70 years ago, it took several decades of relentless efforts to streamline the technique. Ground-based VHE γ-ray astronomy has now established itself as one of the crucial branches of conventional high energy astronomy to study the relativistic Universe. In this article, we look back and present a historical perspective followed by a discussion on the current status and finally what lays ahead.

1 Introduction

Direct detection of γ-rays originating from celestial sources is only possible from space outside the Earth's atmosphere—using either satellite or balloon-borne detectors. The Large Area Telescope (LAT) onboard Fermi γ-ray Space Telescope [1] detects γ-rays up to energies of few hundreds of GeV following pair-production mechanism. At higher energies, the flux of γ-rays arriving at Earth reduces drastically following a power-law spectrum: $\frac{dN}{dE} \propto E^{-\alpha}$ (where $\alpha \sim 2$–3 is the spectral index), which means that the number of photons detected per unit area per unit time falls rapidly with increasing energy. As a result, beyond a few tens of GeV, statistics is not good enough to do γ-ray astronomy with space-borne detectors. At higher energies, one needs large area detectors and longer exposure times. Earth's atmosphere absorbs γ-rays. However, if the γ-rays are energetic enough, with energies above 100 GeV, they interact with the nuclei in the atmosphere and generate a cascade of secondary particles, called Extensive Air Shower (EAS).

Like γ-rays, cosmic rays also produce EAS when they arrive at the top of the atmosphere. Cosmic rays or Astro-particles were discovered in 1912. By the 1950s much of the properties of the EAS were understood. But even after more than 100 years of their discovery, the origin or the sources of cosmic rays are not firmly identified. This is because of the fact that cosmic rays being charged particles, their trajectories bend in the magnetic field of the source environs and interstellar magnetic field en-route including the magnetic field of the Earth. Thus, pointing back the direction of cosmic rays to know their source is not possible unless they are of extremely high energy (EeV, i.e., 10^{18} eV) and of galactic origin. Cosmic rays would interact with matter in the source environs and create neutral species like γ-rays and neutrinos, which could come to Earth directly from the source location without bending their trajectories or losing their direction. Thus, one could use these γ-rays or neutrinos to locate the sources of cosmic rays. In fact, with a desire to search for sources of cosmic rays, the cosmic ray physicists started the work on ground-based γ-ray astronomy, though detecting the γ-rays indirectly, well before the advent of space-based detectors used for direct detection of γ-rays. Alternatively, neutrinos could also point to the source direction. Being weakly interacting particles, in fact, they could come from farther distances compared to γ-rays. However, unlike γ-rays, they are difficult to detect and need massive detectors like IceCube [2], KM3NeT [3], Hyper-Kamiokande [4], etc.

The secondary particles in the EAS, produced by γ-rays, which are mostly electrons and positrons, also get absorbed in the atmosphere, unless the energy of the

[a] e-mail: debanjan.bose@bose.res.in (corresponding author)

γ-ray is high enough ($\sim$ 100 TeV or so) for a sizeable number of charged particles to reach the ground level. In such cases, where the electrons and positrons of the EAS reach the ground level, the shower could be detected by an array of particle detectors. From the relative arrival times of the shower front at different detectors, one can determine the direction of the shower axis in space by the method of triangulation. The shower axis direction is also the arrival direction of the γ-ray.

The secondary charged particles in the EAS also cause the emission of Cherenkov radiation, which is beamed in the forward direction and can reach ground level. Therefore, at energies in the range of a few 10's of GeV to a few 10's of TeV, even though charged particles do not reach the ground, it is possible to detect Cherenkov light and indirectly detect primary γ-ray. This technique, called the atmospheric Cherenkov technique, with the entire atmosphere acting as a detection medium is the most efficient way of detecting very high energy (VHE) γ-rays spanning an energy range of a few 10's of GeV to a few 10's of TeV. For higher γ-ray energies, above 100 TeV, the sizeable number of charged particles reaches the ground and is detected using charged particle detectors. This is ultra high energy (UHE) γ-ray astronomy.

VHE γ-ray astronomy activities started in the 1960s and evolved over the last 60 years. The primary physics objectives of γ-ray astronomy are to establish sites and mechanisms for the origin of cosmic rays and their acceleration to energies way beyond those achieved with man-made accelerators, thereby solving the 100 year old problem of galactic and extragalactic cosmic-ray origin. This is to be done by carrying out multiwavelength and multi-messenger observations of astrophysical sources like supernova remnants, pulsar wind nebulae, active galactic nuclei, etc. Second, exploring how transparent is our Universe, i.e., cosmological studies with TeV γ-rays and understanding the extragalactic background light leading to an estimation of Hubble parameter, thus aiming to constrain the expansion parameters of the Universe. Another topic is Indirect Detection of Dark Matter through observations of dark matter dominated galaxies, thus complementing the ongoing efforts through direct detection techniques and collider searches. Also, there are other points to investigate like the role of cosmic rays in star forming systems, understanding the nature of the central engine in very high energy gamma-ray bursts, probing fundamental physics through studies of Lorentz invariance violation and search for axion-like particles.

In this review, we outline the evolution of the techniques used for the detection of VHE γ-rays, starting from the historical era of the first-generation telescopes (1960–1988), the second generation telescopes after a major breakthrough in the field brought by the Whipple telescope, the third generation, i.e., the present generation telescopes followed by telescopes planned for the future. Even though the main emphasis is on the telescopes based on the atmospheric Cherenkov technique, we also cover other techniques like air shower arrays which are also used for detection of VHE γ-rays. Historical aspects are given in Sect. 2. This is followed by details of the atmospheric Cherenkov technique in Sect. 3. The wavefront sampling telescopes and imaging atmospheric Cherenkov telescopes are discussed in Sects. 4 and 5. Simulations and data analysis technique are explained in Sect. 6. In Sect. 7, we have described the air shower array technique and finally conclusions in Sect. 8.

2 Historical background

Cocconi's proposal in 1960 [5], to search for γ-ray sources by detecting charged particles in EAS using an array of scintillators at the mountain altitudes could be considered as a starting point for ground-based γ-ray astronomy. Another possibility was to use the particular feature of γ-ray initiated showers like paucity of muons in EAS compared to cosmic ray showers. Later, Zatsepin [6] proposed to use Cherenkov light produced by EAS instead of charged particles as proposed by Cocconi. The births of VHE and UHE branches of γ-ray astronomy occurred at the same time.

VHE γ-ray astronomy based on atmospheric Cherenkov technique owes its existence to the pioneering works carried out by Galbraith and Jelley in the early 1950s [7]. They discovered the presence of Cherenkov light in EAS following a suggestion by Blackett to look for Cherenkov light in air [8].

A very first large-scale experiment with twelve 1.5-m-diameter parabolic mirrors on the mount was carried out by a USSR team led by Chudakov at Katsiveli, Crimea in 1960–63 [9] (see Fig. 2 of [10] for photograph of the array). This was followed by a British–Irish experiment at Glencullen, Ireland by Jelley and Porter, having two 90 cm-diameter searchlight mirrors on a Bofors gun mounting [11]. The Smithsonian group in the USA led by G. Fazio built a 10-m-diameter light reflector telescope at Mt. Hopkins at Arizona, USA (Fred Lawrence Whipple Observatory) in 1968 [12]. The early attempts were also carried out by various groups in several parts of the world, viz., USSR, USA, UK, Ireland, Japan, Australia, India, France, Italy, and South Africa. These first-generation experiments were simple and did not have the ability to reject or identify the numerous cosmic ray generated EAS which posed as a background in the detection of γ-rays. Most experiments did not detect any source firmly but detected sources occasionally and some detected transient emissions or sporadic emissions from sources like Crab, Vela, Geminga, X-ray binaries (Cyg X-3, Her X-1, SS-433), and AGNs (Cen-A), etc. None detected consistent steady emission from Crab nebula. (For example, see the review article by Weekes [13] and references therein.) Thus, prospects of ground-based VHE γ-ray astronomy looked bleak due to a very low flux of γ-rays and high cosmic ray background. Nevertheless, the ground-based techniques flourished mainly due to technical difficulties of detecting higher and higher energy photons directly with space-based detectors because

of continuously decreasing γ-ray flux with increasing energy. The effective detection area ($> 10^4$ m^2) offered by the ground-based technique could hardly be realized in detectors deployed in space.

There were lots of efforts to reduce the cosmic ray background and thereby improve the sensitivity for detecting γ-rays as well as to reduce the threshold energy, i.e., the lowest γ-ray energy that can be detected by the experimental system using larger area light collectors, improved electronics, etc. (for a detailed description of sensitivity and energy threshold, see Sect. 6). The discovery of radio pulsar in 1968 [14] offered some method of rejecting a fraction of the cosmic ray background from sources like pulsars and X-ray binaries. The arrival times of cosmic rays are random, while for γ-rays from pulsars are modulated with the pulsar spin frequency. Similarly, arrival times of γ-rays from binary objects (like Cyg X-3) are modulated with orbital frequency. Efforts were also directed toward exploring the subtle differences between cosmic ray initiated EAS and γ-ray initiated ones to reject the vast cosmic ray background. Thus several characteristics like distribution of Cherenkov photons in the light pool of the shower, the time structure of Cherenkov light, the fraction of UV light content in the shower, angular spread of Cherenkov photons within the shower, etc. were being exploited to reduce the cosmic ray background (see for example, review article by Weekes [15] and references therein). An attempt of imaging the shower (albeit a low resolution image) was carried out by Hill and Porter in 1961 using image intensifiers following a suggestion from Jelley in 1958 [16]. The potential advantage of using shower images for discriminating γ-ray-induced showers from those of cosmic rays was listed by Jelley and Porter in a review in 1963 [11]. Early efforts in imaging the shower have been described in an article by Porter [17].

3 Atmospheric Cherenkov technique

As mentioned earlier, the Earth's atmosphere is opaque to γ-rays. However, upon arrival at the top of the atmosphere, a VHE γ-ray produces an electromagnetic shower. Charged particles present in this shower cause atmosphere to emit Cherenkov radiation. These secondary particles or radiation can be detected at the ground level. Telescopes that detect γ-rays by detecting Cherenkov radiation produced in the atmosphere are called Atmospheric Cherenkov Telescopes (ACTs).

When a γ-ray enters into the Earth's atmosphere, it produces an $e^{\pm}$ pair. This pair then emits γ-rays via bremsstrahlung. With successive pair-production and bremsstrahlung, an electromagnetic cascade develops, as shown in Fig. 1. Charged particles, i.e., $e^{\pm}$ pairs present in this cascade travel with a speed more than the speed of light in the medium and therefore cause emission of Cherenkov radiation peaking in the UV-blue region of the visible spectrum, lasting for a few ns. This radiation is very faint and emitted in a small angle ($\sim 1^\circ$ in the atmosphere) in the forward direction (see Fig. 2). The forward direction and coherent nature of this radiation enable one to determine the arrival direction of the incident γ-ray accurately. Cherenkov photons are spread over a large circular area with a diameter in the range of 100–120 m on the ground. One or multiple telescopes located anywhere in this light pool can detect the incident γ-ray indirectly by detecting Cherenkov photons. Hence, effective area for these telescopes is of the order of 10^4 to 10^5 m^2.

These telescopes or ACTs are essentially made up of an optical reflector i.e. a mirror to collect the Cherenkov light and one or more Photo Multiplier Tubes or PMTs at the focus of the reflector. PMTs are the ideal detectors for this purpose because of their high gain, low noise, and ultra-fast (ns) response. Also, their spectral response matches with the Cherenkov spectrum. These telescopes are equipped with very fast front-end electronics to process electrical signals produced by the PMTs.

There are two types of backgrounds that pose a challenge for ground-based γ-ray astronomy: EAS generated by cosmic rays (mostly proton primaries) and night sky background (NSB). For every γ-ray initiated EAS, there are about 1000 cosmic ray initiated EAS, which can be detected by ACT.

Cosmic rays initiate a cascade by collision with atmospheric nuclei, resulting in the production of short-lived pions which include neutral pions and charged pions. Neutral pions decay into γ-rays and charged pions produce muons via decay along with other particles. These γ-rays and decay products of muons constitute an electromagnetic component of EAS (Fig. 1). All these charged particles produce Cherenkov radiation. Therefore, basically, mechanisms for emission of Cherenkov light are identical for γ-ray and cosmic ray initiated EAS. Thus, the success of any ground-based telescope hinges upon how well it can distinguish a γ-ray initiated shower from a cosmic ray or a hadronic shower. Because of the differences in the development of air showers initiated by γ-ray and cosmic ray, there are some subtle differences in Cherenkov light distribution produced by them on the ground. γ-ray showers can be separated from hadronic ones by comparing their Cherenkov light pattern.

The Cherenkov radiation emitted by secondary charged particles in EAS is very faint compared to NSB. Therefore, ACTs can only be operated at a dark site, away from man-made light pollution, during moonless nights with clear weather. The number of NSB photons is typically of the order of 10^{12} photons/m^2/s/sr, several orders of magnitude higher compared to the number of Cherenkov photons. For example, the number of Cherenkov photons produced by a γ-ray of energy 1 TeV is only of the order of a few hundreds per m^2 at 2 km altitude a.s.l. These NSB photons peak at higher wavelengths compared to Cherenkov photons as shown in Fig. 3 and are incoherent. NSB can be suppressed by several orders by selecting PMTs whose quantum efficiency peaks in the wavelength range 300–400 nm, selecting a narrow time window ($\sim$ few tens of

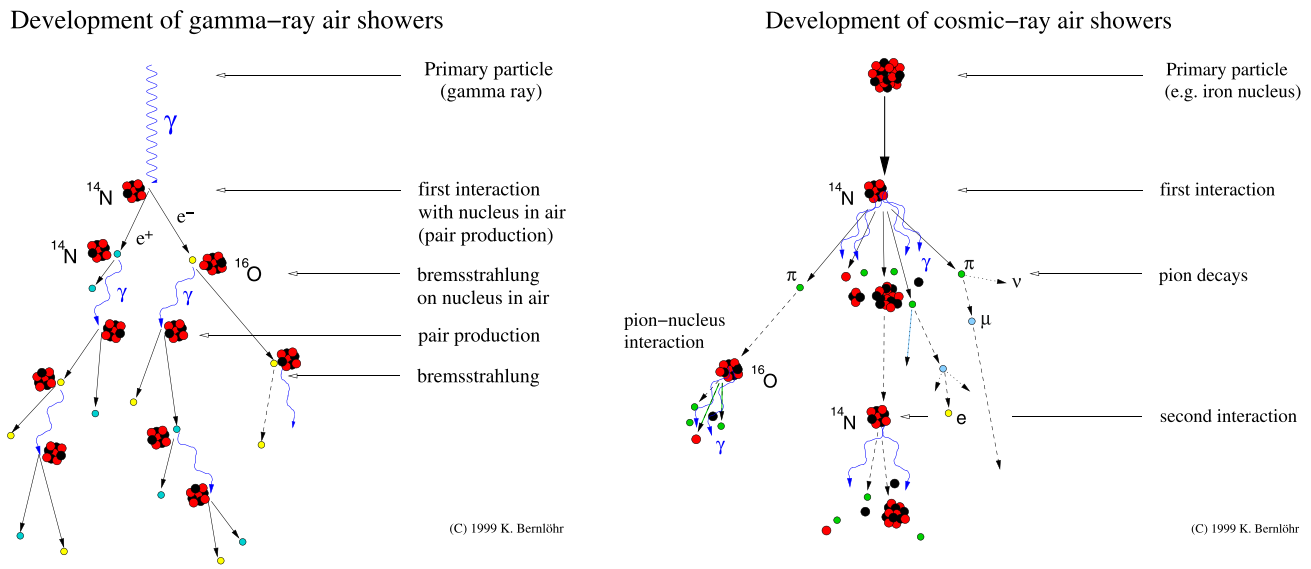

Fig. 1 EAS initiated by a γ-ray (left) and a cosmic ray (right). γ-ray produces electromagnetic cascade, whereas cosmic ray produces three overlapping cascades: electromagnetic, pionic, and nuclear. Reproduced from https://www.mpi-hd.mpg.de/hfm/CosmicRay/Showers.html with permission from author Konrad Bernlöhr

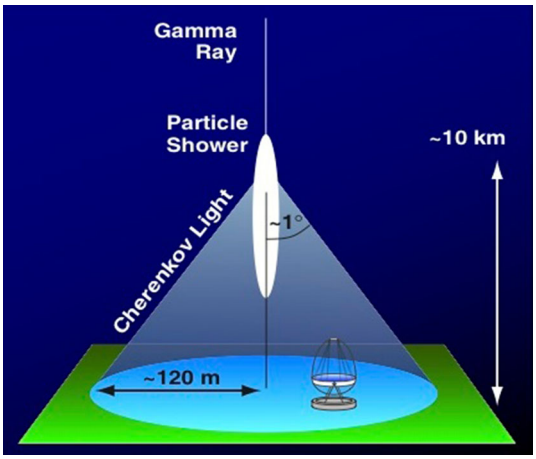

Fig. 2 Principle of atmospheric Cherenkov technique. Celestial γ-ray generates electromagnetic shower in atmosphere. Secondary charged particles in the shower cause atmosphere to emit Cherenkov radiation in a small cone. Cherenkov photons create a light pool on the ground spread over a circular area of radius $\sim$ 120 m. This light is detected using Atmospheric Cherenkov Telescope (ACT). (Reproduced from [18] with permission from authors de Naurois and Mazin)

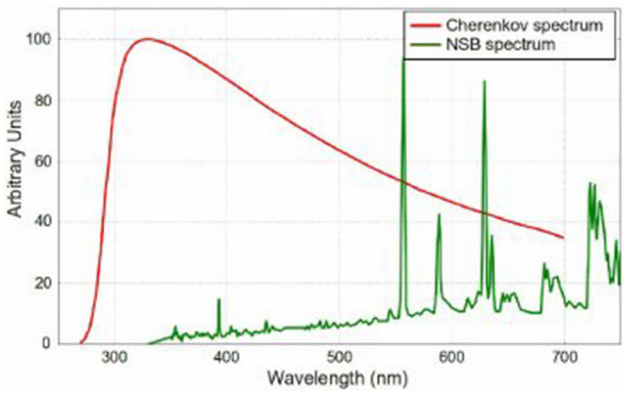

Fig. 3 Distribution of Cherenkov photons (red) and night sky background photons (green) w.r.t. wavelength, measured at La Palma, Canary Island, Spain. Reproduced with permission from [19], the plot is generated using the data from [20]

ns) for charge integration and by allowing coincidences between multiple pixels or telescopes.

There are two types of techniques used to detect a γ-ray signal from an astrophysical source, namely the wavefront sampling technique and the imaging technique. The wavefront sampling technique is the older one and has been extensively used in the past. However, in the last 20 years, it has been shown that the imaging technique is a more powerful tool to detect VHE γ-rays on the ground due to superior rejection of cosmic ray produced background. In the following sections, both these techniques are discussed in detail.

3.1 Wavefront sampling technique

In the wavefront sampling technique, multiple collectors sample light from across the Cherenkov pool. In this technique, the shower is sampled in the horizontal plane. An array of reflectors is spread across long-baseline with one or more PMTs in the focal plane of each reflector. These reflectors record arrival times of Cherenkov shower front and density of photons at several points in the light pool (see Fig. 4). Using arrival time information, the Cherenkov shower front can be

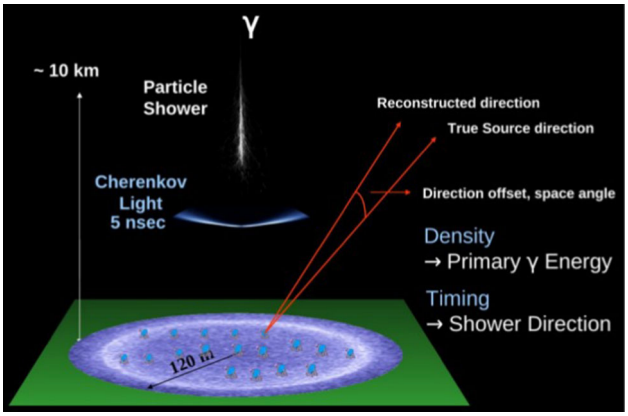

Fig. 4 Wavefront sampling technique with multiple collectors sampling light from across Cherenkov pool

reconstructed. This in turn gives the arrival direction of the incident γ-ray. The photon density from various PMTs can be used to reconstruct the lateral density profile of Cherenkov light in the shower. This also gives an estimate of the total Cherenkov yield of the shower which is proportional to the energy of the incident γ-ray primary.

3.2 Imaging technique

The most successful technique to detect Cherenkov light from EAS is to make so-called "pictures" of the showers. The telescopes which employ this technique are called Imaging Atmospheric Cherenkov Telescopes (IACTs). These telescopes consist of large reflectors which focus the Cherenkov light from air showers onto a focal plane where a camera is placed. The diameters of the reflectors used in various telescopes are in the range of 4–28 m. The reflector consists of spherical, hexagonal, or square mirror facets made up of glass or aluminium. The typical size of mirror facets is about 0.5–1 m and there are about a few hundred mirror facets in a medium-size (10–12 m diameter) telescope. These mirror facets are arranged generally in the form of Davies–Cotton or paraboloid design. Davies–Cotton configuration is simpler in design with identical mirror facets and straightforward alignment procedure, have inferior on-axis and superior off-axis focusing. On the other hand, the paraboloid design is slightly difficult to manufacture and align as all facets have different radii of curvature, has superior on-axis and inferior off-axis focusing. Davies–Cotton design has another drawback of the requirement of longer integration times for images as light from various parts of the reflector reaches the focal plane at different times. Whereas for paraboloid design, light from different parts of the reflector reaches the focal plane simultaneously, thereby reducing integration time for images. So typically, Davies–Cotton design is common for small- or medium-size telescopes up to about 12 m diameter, whereas larger telescopes are mostly based on paraboloid design.

The camera in the focal plane of IACT comprises many PMTs, which act as pixels. A typical field of view of a camera is 3°–5° as the size of Cherenkov image is typically around a degree. Normally, light concentrators are mounted in front of each PMT pixel to increase collection area by taking care of dead space between the PMTs as well as to cut off stray light falling on the camera. Typical pixel size varies in the range of 0.1°–0.3° and typically there are 500–1000 pixels in the camera of medium-size telescope with a diameter of $\sim$ 12 m. The camera records an image of the shower, and several properties of the image, for example, its shape, intensity, and orientation, allow one to determine the properties of the shower primary (see Fig. 5).

4 Wavefront sampling telescopes

As mentioned earlier, the wavefront sampling technique is an older technique used for the detection of Cherenkov photons. Some of the examples from past generation experiments based on this technique are the Pachmarhi Array of Cherenkov Telescopes (PACT) and the Tracking High Energy Muons In Showers Triggered On Cherenkov Light Emission (THEMISTOCLE) experiment. PACT was a multi-telescope array in central India at an altitude of 1075 m [21]. There were 24 telescopes spread over an area of 80 m $\times$ 100 m. Each telescope consisted of seven 90-cm-diameter parabolic mirrors with PMT mounted at the focal point of each mirror. THEMISTOCLE experiment was located at THEMIS solar power plant site near Font-Romeu in the eastern French Pyrenees [22]. There were 18 telescopes, each having an 80-cm-diameter parabolic mirror and a single PMT at the focus. These telescopes were distributed over the roughly elliptical 200 m $\times$ 300 m area. Another array of seven larger, 7-m-diameter reflectors, called AStronomie GAmma a Themis (ASGAT), was also operated near THEMISTOCLE [23]. All these experiments had energy thresholds close to a few hundred GeV or higher, (PACT: $\sim$ 750 GeV, THEMISTOCLE: $\sim$ 3 TeV, ASGAT: $\sim$ 500 GeV).

Around the same time, a few solar array experiments like Solar Tower Atmospheric Cherenkov Effect Experiment (STACEE) [24], Cherenkov Low Energy Sampling and Timing Experiment (CELESTE) [25], and Gamma-Ray Astronomy at ALmeria (GRAAL) [26] were built with the aim of reducing energy thresholds to bridge the gap between space-based and ground-based detectors. All these experiments used large heliostats of solar power facilities to collect more Cherenkov photons to reduce the energy threshold. Light from heliostats was reflected onto secondary mirrors located inside a tower, which then focused light onto a camera consisting of multiple PMTs (see Fig. 6). STACEE was located in Albuquerque, New Mexico, USA, CELESTE in the French Pyrenees and GRAAL was located in Almeria, Spain. Due to the larger mirror area, these arrays could achieve energy thresholds in the range of 60–250 GeV. Details of these wavefront sampling arrays are given in Table 1.

As mentioned earlier, cosmic rays form a huge background against which γ-ray signal is to be detected.

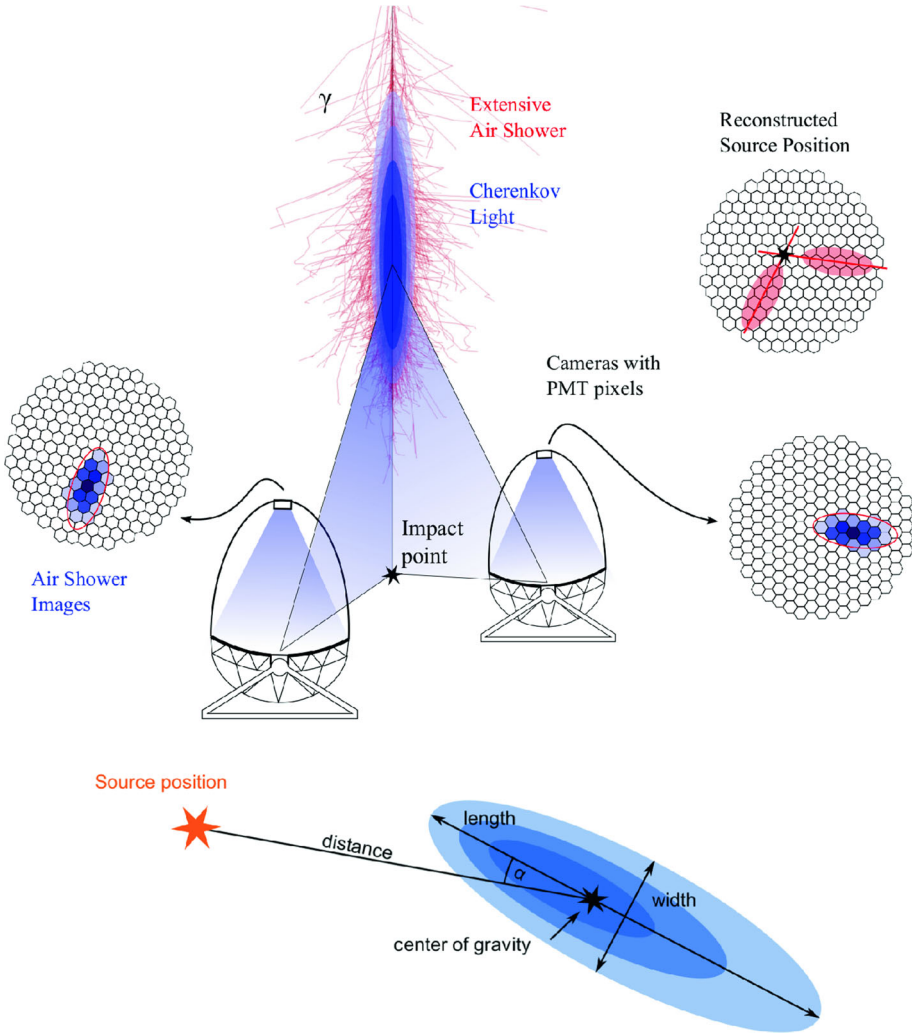

Fig. 5 A schematic view of stereoscopic observations of two imaging telescopes. The lower figure shows the shower image parameters based on a moment analysis. The image of the shower is fitted by an ellipse where the semi-major and semi-minor axes are the length and width parameters, and represent the 'shape' of the image. The alpha parameter is used to estimate the orientation or the pointing of the image. The authors acknowledge the MAGIC collaboration for providing this diagram

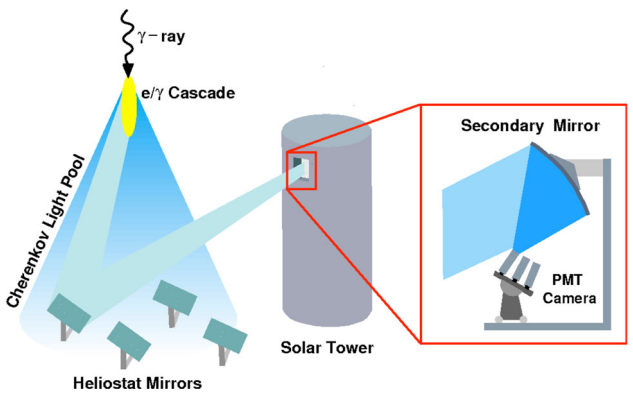

Fig. 6 Solar array experiments where Cherenkov photons are reflected by heliostat mirrors towards secondary mirrors located inside the tower. These secondary mirrors focus Cherenkov light onto an array of PMTs. Image is reproduced with permission from [27]

This is achieved in the wavefront sampling technique by rejecting off-axis showers which are produced by cosmic rays. Apart from this, some Gamma-Hadron Segregation (GHS) criteria are also used. For example, higher fluctuations in cosmic ray showers compared to γ-rays arising from shower kinematics were used by CELESTE, to get moderate rejection [28]. Slightly better rejection was obtained by CELESTE and STACEE using the shapes of the pulses recorded by flash-ADCs. In this method, pulses from various telescopes were shifted and added together after considering arrival time delays. A parameter that defines the ratio of height and width of the summed signal was used for selecting γ-ray showers (H/W) as distribution of H/W is narrower for γ-rays compared to cosmic rays [29]. Sources like Crab nebula, which is also considered as a standard candle in VHE γ-ray astronomy, blazar class Active Galactic Nuclei (AGNs) like Mrk 421 were successfully detected by these arrays [28,30–32]. Overall, it turned out that the GHS criteria used in the wavefront sampling technique are less efficient compared to the imaging technique as we will see later in this review. Hence, slowly imaging technique became more popular, and is currently the most advanced and preferred option to detect VHE γ-rays from celestial sources.

Table 1 List of telescopes designed based on wavefront sampling

Name	Place	Altitude	Array type	Energy threshold	Duration Start–end
ASGAT	French Pyrenees, France	1650 m	7 telescopes	500 GeV	1989–1995
THEMISTOCLE	French Pyrenees, France	1650 m	18 Telescopes	3 TeV	1990–1995
PACT	Pachmarhi, India	1075 m	24 telescopes	750 GeV	2000–2012
CELESTE	French Pyrenees, France	1650 m	Heliostat Array 53 telescopes	60 GeV	1999–2004
STACEE	Albuquerque, New Mexico, USA	1705 m	Heliostat Array 64 telescopes	150 GeV	2001–2007
GRAAL	Almeria, Spain	505 m	Heliostat Array 63 telescopes	250 GeV	1998–2001
HAGAR	Hanle, India	4270 m	7 telescopes	210 GeV	2008–..

Presently, only one wavefront sampling array, High-Altitude GAmma-Ray (HAGAR) telescope system is operational. It is an array of seven small size telescopes, operated at a high-altitude location called Hanle in the Ladakh region of the Himalayas in India since 2009 [33]. Each of these telescopes has seven para-axially mounted parabolic mirrors of diameter 0.9 m (see Fig. 7). The altitude of Hanle is 4270 m a.s.l. and HAGAR is the first atmospheric Cherenkov telescope to be operated at such a high-altitude location. High-altitude location was chosen as a cost effective way to achieve a lower energy threshold with a moderate-size telescope. The energy threshold depends on the number of Cherenkov photons collected by the reflector. Therefore, one way of reducing the energy threshold is to use a large-size reflector. Whereas alternative way is to install a telescope at high-altitude location. Cherenkov photon density is higher at higher altitudes and atmospheric absorption of Cherenkov photons is less, which reduces the energy threshold of the telescope. Taking advantage of high-altitude location, HAGAR could achieve the energy threshold of $\sim$ 210 GeV. This is about a factor of four reduction compared to similar (in fact, larger) array PACT which was operated at an altitude of 1 km.

5 Imaging atmospheric Cherenkov telescopes

The imaging technique has been in use for more than 30 years and has evolved with time. In this section, we summarise the past-, present-, and future-generation IACTs.

5.1 Past-generation IACTs

The observations of very high energy gamma rays using the imaging technique was pioneered by the Whipple telescope collaboration. This is the same 10-m-diameter reflector used by the group led by G. Fazio earlier. It was located at Mount Hopkins, Arizona at an altitude of 2300 m a.s.l. The reflector was composed of 248 hexagonal aluminized and anodized glass mirror facets mounted in Davies–Cotton design (see Fig. 8). Mirror facets had radius of curvature of 14.3 m and were mounted on a 7.3-m radius spherical support structure. Based on the idea of using matrices of PMTs as a camera to image Cherenkov light from air showers from Weekes and Turver [35], a 37-pixel camera was installed in the focal plane of the reflector. Through Monte Carlo simulations Hillas identified the so-called Hillas parameters, which are image parameters, to discriminate γ-rays from huge cosmic ray background [36]. Using these GHS parameters, 98% of the background was rejected and Crab nebula was detected at a statistical significance of 9 σ at energies above 700 GeV [37]. Whipple continued operation till 2006. Over the years, imaging camera went through several transformations

Fig. 7 Seven-element HAGAR telescope array located at Hanle in India at an altitude of ~ 4.3 kms asl. Photo credit: HAGAR group

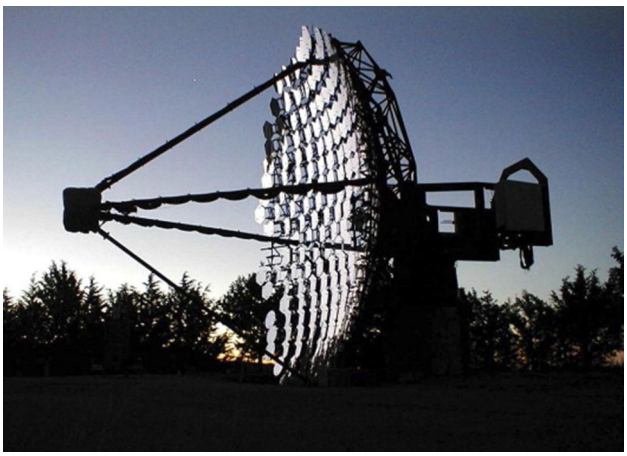

Fig. 8 Whipple 10-m imaging atmospheric Cherenkov telescope. Reproduced with permission from [34]

with a steady increase in the number of pixels. In the final configuration, there were 379 pixels. Apart from Crab nebula, Whipple discovered VHE γ-ray emission from four blazar class AGNs: Markarian 421 in the year 1992 [38], Markarian 501 in 1996 [39], 1ES 2344+514 in 1998 [40], and H1426+428 in 2002 [41].

Few years after Whipple discovered emission from Crab nebula, another IACT called Cherenkov Array at Themis (CAT) was built in France. Though, using a smaller reflector compared to Whipple, with a diameter of about 5 m, CAT could achieve performance comparable to that of Whipple because of finer pixel camera consisting of 546 PMT pixels of 0.12° size and 54 larger PMTs in two guard rings, covering a total FOV of 4.8° [42].

The next milestone in the atmospheric Cherenkov technique was achieved by extending the technique to an array of telescopes. This is called "stereoscopy". This approach was demonstrated by High Energy Gamma-Ray Astronomy (HEGRA) experiment located at La Palma in Canary Islands at an altitude of 2200 m a.s.l. This air shower array also had IACT system embedded, consisting of an array of five telescopes. Telescope installation started in 1992 and went through various stages including refurbishing, and by September 1998, entire system consisting of five telescopes was operational [43]. Each of these telescopes had 8.5 m^2 mirror reflector area and camera consisting of 271 PMT pixels. Telescopes were arranged at the corners of a square with a side length of 100 m and one telescope at the centre. HEGRA pioneered the stereoscopic observation technique providing multiple images of a given air shower from various directions. This provided a better reconstruction of shower direction and shower core position, thereby improving angular resolution, GHS, and energy resolution. HEGRA telescope system was operational till September 2002 and apart from successfully detecting VHE γ-ray emission from known VHE emitters like Crab nebula [44] and blazars including Mrk 421, Mrk 501, 1ES2344+514, and H1426+428, it discovered sources like Cas A (shell type supernova remnant) [45], TeV J2032+4130 (a binary system) [46], and M 87 (radio galaxy) [47].

Whipple, CAT, and HEGRA were second-generation atmospheric Cherenkov telescopes, which along with some other telescopes like GT-48 [48], 7 Telescope Array [49], Durham Mark-6 [50], CANGAROO-I [51], Shalon [52], etc., as well as some of the telescopes based on wavefront sampling technique, firmly established γ-ray astronomy as legitimate branch of astronomy and

paved the way for next-generation telescopes. Some of the details of these telescopes are listed in Table 2.

5.2 Present-generation IACTs

After the successful operation of Whipple demonstrating the power of imaging technique, CAT showing advantages of fine pixellated camera, and HEGRA successfully displaying significant improvements in sensitivity and primary energy estimation with stereoscopy, various groups moved to next generation of IACTs. The aim was to improve the sensitivity and to reduce the energy threshold to 100 GeV or less to have overlap with satellite-based detectors like Fermi-LAT. These third-generation telescopes combined all three aspects like large reflector size, camera with fine pixels, and stereoscopic operations. Four such stereoscopic arrays came into operation since 2003. These include 4-telescope arrays H.E.S.S., CANGAROO-III, and VERITAS and 2-telescope array MAGIC.

5.2.1 H.E.S.S.

The High Energy Stereoscopic System[1] (H.E.S.S.) is an array of four telescopes located at Gamesberg Mountain in Namibia at an altitude of 1800 m a.s.l. (see Fig. 9). Each of these telescopes has a 12-m-diameter reflector based on Davies–Cotton design. Each reflector consists of 382 round mirror facets of 60 cm diameter. The focal length of each telescope is 15 m and 980-pixel camera is mounted in the focal plane. The size of each pixel is 0.16° and the camera covers the field of view of about 5°. The angular resolution of H.E.S.S. is estimated to be 0.1° and the energy threshold is in the neighbourhood of 100 GeV. H.E.S.S. can detect γ-ray flux equivalent to 1% of Crab in 25 h of observation [53]. This is almost an order of magnitude improvement over the previous generation telescopes.

H.E.S.S. array is operational since 2003. This was the first telescope array with good sensitivity operating in the Southern hemisphere. It carried out the first high resolution and sensitive survey of the Milky way in TeV γ-rays [54]. It discovered more than 100 objects of diverse classes. Another interesting measurement from H.E.S.S. is that of the energy spectrum of cosmic electrons above 600 GeV, taking advantage of a very large collection area offered by atmospheric Cherenkov technique compared to direct measurements by satellite or balloon-borne detectors [55].

In 2012, the next phase of H.E.S.S. consisting of a single telescope with a 28-m-diameter reflector was installed. This is the largest atmospheric Cherenkov telescope in the world. It has a parabolic reflector and camera consisting of 2048 pixels (see Fig. 10 for camera picture). Taking advantage of the lower energy threshold achieved due to the large reflector size, this telescope could detect Vela pulsar from sub-20 GeV to 100 GeV energy range successfully [56]. This is the first

[1] https://www.mpi-hd.mpg.de/hfm/HESS/.

Table 2 List of telescopes designed based on imaging technique

Name	Place	Altitude	No. of telescopes	Mirror size	No. of pixels	F.O.V.	Energy threshold	Duration Start–end
Whipple	Arizona, USA	2300 m	1	10 m	379	2.8°	300 GeV	1985–2006
GT-48	Crimea, Ukraine	600 m	2	4 × 1.2 m	150	2.6°	1 TeV	1989–2010
SHALON	Tien Shan, Kazakhstan	3340 m	2	3.6 m	144	8°	800 GeV	1992–..
CAT	French Pyrenees, France	1650 m	1	4.9 m	546	4.8°	250 GeV	1996–2002
7 Telescope Array	Utah, USA	1600 m	7	3 m	256	4°	600 GeV	1997–1999
HEGRA	Canary Islands, Spain	2200 m	5	3.4 m	271	4.3°	500 GeV	1992–2002
CANGAROO-I	Woomera, Australia	160 m	1	3.8 m	256	2.9°	2.7 TeV	1991–1998
CANGAROO-III	Woomera, Australia	160 m	4	10 m	427	4°	200 GeV	2004–2011
H.E.S.S. I	Khomas highlands, Namibia	1800 m	4	12 m	960	5°	160 GeV	2003–..
H.E.S.S. II	Khomas highlands, Namibia	1800 m	1	28 m	2048	3.2 °	30 GeV	2012–..
VERITAS	Arizona, USA	1268 m	4	12 m	499	3.5°	85 GeV	2007–..
MAGIC	Canary Islands, Spain	2200 m	2	17 m	1039	3.5°	50 GeV	2004–..
TACTIC	Mt Abu, India	1300 m	4	3.6 m	349	6°	850 GeV	2001–..
FACT	Canary Islands, Spain	2200 m	1	3.4 m	1440	4.5°	750 GeV	2011–..
MACE	Hanle, India	4270 m	1	21 m	1088	4°	20 GeV	2021–..

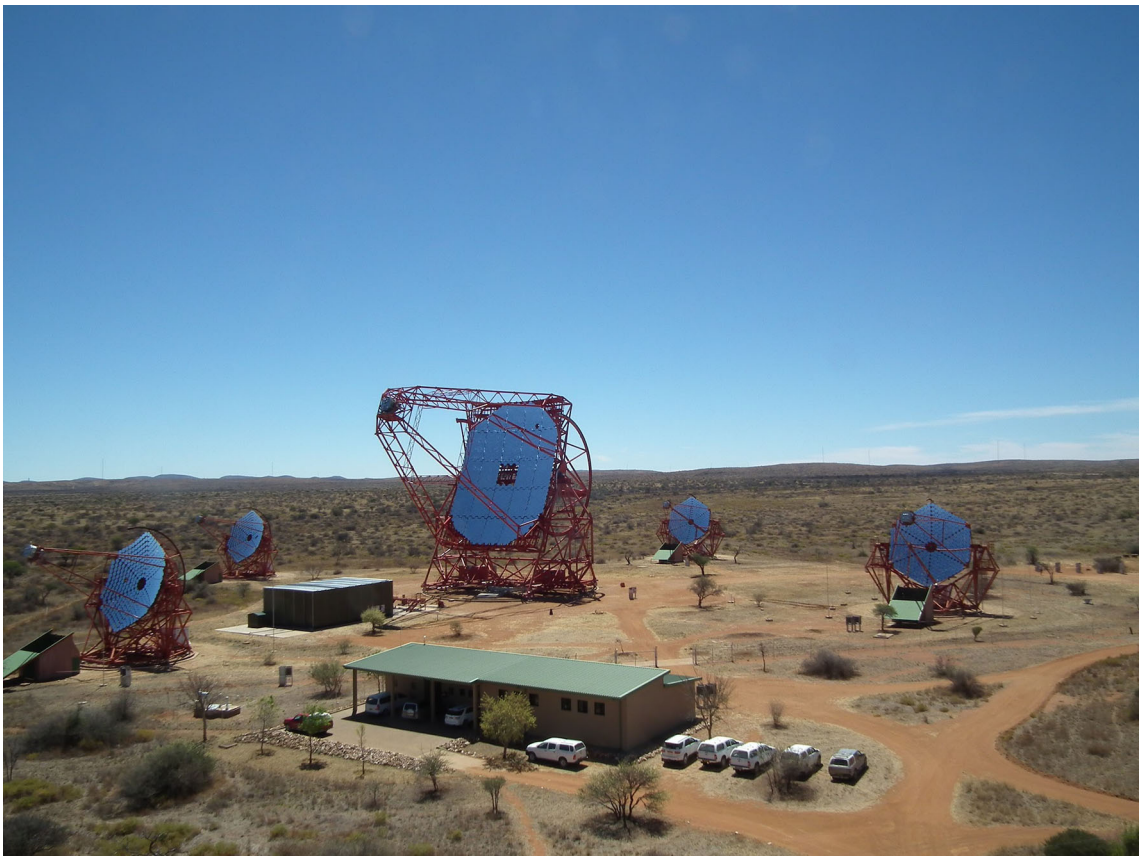

Fig. 9 H.E.S.S. IACT array at Gamesberg in Namibia, consisting of four 12-m-diameter and one 28-m-diameter telescope. Picture courtesy: H.E.S.S. collaboration

time, measurements are reported from ground-based atmospheric Cherenkov telescopes for this object.

5.2.2 MAGIC

The Major Atmospheric Gamma Imaging Cherenkov[2] (MAGIC) telescope is a system of two 17-m-diameter IACTs (see Fig. 11) located in El Roque de los Muchachos observatory in Canary Islands of La Palma at an altitude of 2200 m a.s.l.

These telescopes are designed in such a way that their lower parts, like undercarriage and bogeys which move only in the azimuth direction, are made up of steel. Whereas the lightweight upper parts such as the mirror support are made up of carbon fibre-reinforced plastic tubes. This unique state-of-the-art design helps MAGIC telescopes to orient themselves by 180° in the azimuth direction in about 25 s. MAGIC uses parabolic mirrors to reflect Cherenkov photons. The mirror surface is segmented in nature and is comprised of smaller units of 0.5–1 m^2.

A single MAGIC camera comprises of 1039 PMTs of Hamamatsu type R10408, 25.4 mm diameter and typical quantum efficiency of around 32%. The PMTs or pixels are grouped in seven PMTs to build a modular unit. Each pixel has an FoV of 0.1° and the FoV of the MAGIC camera is 3.5° (for details about the hardware of the MAGIC telescope system, see [57]).

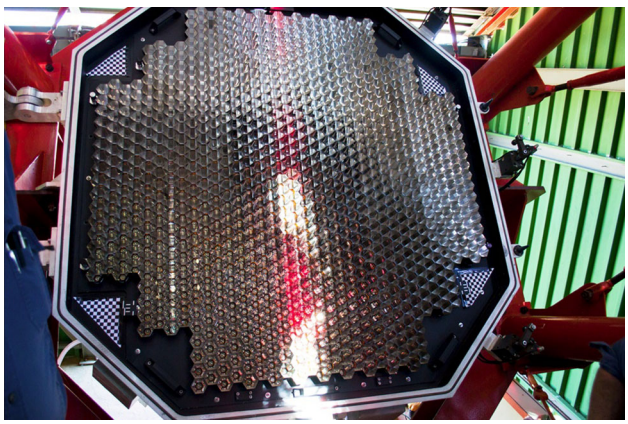

Fig. 10 Photograph of the H.E.S.S. II camera, consisting of 2048 pixels. Picture credit: Derek Duckitt, Hermanus Astronomy Centre, South Africa

Observations of the Crab Nebula were performed at low zenith angles to estimate the key performance parameters of the MAGIC stereo system. For these observations, the standard trigger threshold of the MAGIC telescopes is ∼ 50 GeV. The integral sensitivity for point-like sources with Crab Nebula-like spectrum

[2] https://wwwmagic.mppmu.mpg.de.

Fig. 11 MAGIC telescope system at La Palma in the Canary Islands consisting of two 17-m-diameter telescopes. Picture courtesy: MAGIC collaboration

above 220 GeV is (0.66 ±0.03)% of Crab Nebula flux in 50 h of observations [58].

The large size of MAGIC and its very fast repositioning scheme enables it to focus on observations of distant AGNs and GRBs as well as pulsars. MAGIC is the first TeV telescope to have detected pulsations from the Crab with a high significance at energies greater than 25 GeV [59,60]. Other significant detections include the first ever detection of TeV γ-ray photons from GRB 190114C [61] by an IACT, detection of a burst of photons at TeV energies from a candidate neutrino blazar (TXS0506+056) [62], and detection of high energy γ-rays from two of the most distant AGNs known, PKS1441+25 [63] and QSO B0218+357 [64]. At the highest energies, taking advantage of very large zenith angle observations, MAGIC has been able to detect γ-rays up to 100 TeV from the Crab nebula [65].

5.2.3 VERITAS

The Very Energetic Radiation Imaging Telescope Array System[3] (VERITAS) is a ground-based γ-ray telescope array operating at Fred Lawrence Whipple Observatory (FLWO) in southern Arizona, USA. It is an array of four 12-m-diameter reflectors (see Fig. 12) designed to perform γ-ray astronomy of celestial sources in the energy range of approximately 100 GeV to several tens of TeV. Each telescope of VERITAS is based on an alt-azimuth positioner system with a maximum slew speed of about 1°/s. The pointing accuracy of a VERITAS telescope is typically better than ±0.01°. The optical system of the telescope is based on Davies Cotton design and consists of about 350 identical hexagonal spherical mirrors of 30 cm^2 each having a radius of curvature of about 24 m. Each mirror facet is made from glass, slumped, polished, and then aluminized and anodized.

The camera of the telescope is located at the focal plane of the telescope and has a dimension of about 1.8 m × 1.8 m. The camera is equipped with 499 circular PMTs, giving an angular pixel spacing of 0.15° and a total FoV of 3.5°.

VERITAS employs a three-tier trigger system to reduce the rate of several background events. The first trigger system works on the single-pixel level, the second checks for specific patterns of single-level pixels within a certain time window, and the third works as regards to telescope coincidence, requiring simultaneous observations of an air-shower event in at least two of the four telescopes (ensuring a "stereoscopic" view of the event). The angular resolution of VERITAS (68% containment radius) is 0.08° at 1 TeV and it worsens to about 0.13° at 200 GeV. The energy resolution is about 17% at 1 TeV and the point source sensitivity is about 1% of the Crab nebula flux in less than 25 h.

VERITAS carried out the first high-resolution scan of the Cygnus region in the northern hemisphere and discovered a few sources in the region [66–68]. Apart from that, one of the main highlights of the VERITAS discovery program has been the detection of a starburst galaxy M82 [69]. Besides these interesting discoveries, it has also discovered a few AGNs at moderate-to-high redshifts [70–72] and also the Crab pulsar [73] at energies up to several hundreds of GeV.

5.2.4 Other IACTs

The Collaboration between Australia and Nippon for a GAmma-Ray Observatory in the Outback (CANGAROO-III), a stereoscopic array of imaging telescopes, was operated at Woomera in Australia at an altitude of 165 m a.s.l. during 2004–2011 [74]. This was an array of four telescopes with a reflector diameter

[3] https://veritas.sao.arizona.edu

Fig. 12 VERITAS array in Arizona consisting of four 12-m-diameter telescopes. Picture courtesy: VERITAS collaboration

of 10 m. One moderate-size telescope, TeV Atmospheric Cherenkov Telescope with Imaging Camera (TACTIC) is operational at Mt Abu, in Western India since 2001 [75]. It has a 4-m-diameter reflector with 349-pixel camera.

Another large-size telescope based on imaging technique, Major Atmospheric Cherenkov Experiment (MACE), is recently commissioned at Hanle [76] in the Himalayas, India. The diameter of its reflector is 21 m and it has a camera consisting of 1088 pixels. Science observations with MACE are expected to commence soon. Based on the simulations, MACE is expected to achieve an energy threshold of ~ 20 GeV, taking advantage of high-altitude location as well as the large size of the reflector.

The First g-Apd Cherenkov Telescope (FACT) [77] is the first IACT using Geiger-mode avalanche photodiodes (G-APDs) or silicon photomultipliers (SiPMs) as photo-sensors instead of usual PMTs. SiPMs have several advantages over PMTs, like higher photon detection efficiency, lower operating voltage, etc. Most importantly, unlike PMTs, they can be safely operated in a bright environment. Therefore, it is possible to increase the observation duty cycle by operating a telescope in the moon-lit part of the night partially. FACT is a moderate-size telescope with about a 4-m-diameter reflector. In fact, it is one of the mounts from the HEGRA telescope array which is refurbished. Its camera consists of 1440 pixels of SiPMs with solid light concentrators mounted in front, to take care of dead space between the pixels. FACT is operational since 2012 and has observed several sources, largely blazar class AGNs and provided long duration observations for these sources. This has paved a way for the usage of SiPMs in future-generation telescopes.

5.3 Future IACTs: CTA

Cherenkov Telescope Array[4] (CTA) project is a next-generation array of IACTs aimed at making measurements of the γ-ray sky with unprecedented details over a wide energy range from 20 GeV to $\sim$ 300 TeV [78]. CTA will consist of two IACT arrays, one in the southern hemisphere which will primarily focus on galactic γ-ray sources and the other in the northern hemisphere which will focus more on extragalactic sources. The expected sensitivity of CTA will be at least one order of magnitude better than any existing IACTs. CTA with its improved angular & energy resolutions and wide field of view will study γ-ray sources with high precision.

These arrays would allow for both deep field investigations and surveys in parallel with monitoring of the brightest known variable sources and activity related to alerts from space-based instruments in other wavelengths. The site in the southern hemisphere is Paranal, Chile and the site in the northern hemisphere is La Palma, Canary Islands, Spain. The two sites will allow for a full sky coverage and consequently access to many more γ-ray sources with the possibility of discovering many rare source classes and rare events, such as GRBs or supernova explosions [79].

To reach the performance goals as mentioned above and specifically the wide energy range to be covered, the design of the telescope array is required to be optimized for three adjacent energy ranges:

The low energy range ≤ 100 GeV: To detect γ-rays down to a few tens of GeV, the Cherenkov light needs to be sampled efficiently as the various discriminating parameters between a γ-ray-induced shower and a hadron-induced shower start to overlap at energies

[4] https://www.cta-observatory.org/.

below 100 GeV. This creates a huge background in the data, and thus, systematic uncertainties of the background estimation limit the sensitivity of the instrument. This problem can be overcome with the deployment of a few closely packed large-size telescopes to collect as many photons as possible from the low energy showers.

The core energy range 0.1–50 TeV: Shower detection and reconstruction in this energy range has been the bread and butter of the current instruments. The sensitivity in this energy range can be further improved by the deployment of an array of mid-size telescopes of about 12-m diameters with a spacing of about 100 m. The array size for the first time will cover the entire Cherenkov pool which will improve the sensitivity due to the increased collection area of the array and also due to higher quality reconstruction of the shower parameters, since individual showers will typically be stereoscopically imaged by a large number of telescopes compared to a single large telescope or a few medium-size telescopes.

The high energy range > 50 TeV: At the highest energies, the main limitation is the number of detected γ-ray showers due to the steeply falling flux. Hence, there is a need for covering an area of several square kms. Deployment of an array of many small telescopes (~ 4 to 6 m class) over a large area will extend the energy range beyond 300 TeV, a range where most imaging Cherenkov telescopes have never been operated.

It is clear from the current the knowledge of operation of Cherenkov telescopes that a mixed array is required to achieve the best sensitivity over a wide energy range spanning over 4 decades in energy. Figure 13 shows the artistic illustration of the proposed CTA. The main design drivers to cover the energy ranges mentioned above are the following:

Large-Size Telescopes (LST): A few large telescopes (23-m-diameter class) with relatively narrow FoV [5] and fine pixelization ($\sim 0.1^\circ$) with close spacing will enable one to access the lowest energies possible and thus allow for detection of AGNs at high redshifts and galactic sources like pulsars which exhibit strong spectral cutoffs at lower energies (few tens of GeV typically). Furthermore, at these energies, we will have a good overlap with satellite-based γ-ray detectors like Fermi-LAT. The construction of the prototype LST [80] is complete, and it has been installed at La Palma, Canary Islands, Spain, on the CTA observatory site of the Observatorio del Roque de los Muchachos. It is currently being commissioned and is foreseen to become the first CTA telescope at the site (see Fig. 14).

Medium-Size Telescopes (MST): In the known energy range between 100 GeV and 50 TeV, where most of the current installations are operating, an extended array covering an area of few km^2 is required for increased collection area providing a higher proportion of events which would be contained within the array and would thus have excellent energy and angular resolution leading to increased sensitivity. An array with few tens of telescopes of medium sizes (12-m-diameter class) with wide FoV (6°–8°) for studying morphologies of extended objects and moderate pixel size of 0.18° in under construction. Currently, a prototype MST has been built and several key parameters of the telescope are being studied in detail. The camera of the prototype consists of about 1800 pixels with an FoV of 7.7 deg. The readout system is based on the philosophy called *FlashCam* where the trigger and readout system are fully digital based on FADCs and FPGAs as key components of front-end electronics [81]. An alternative camera based on the philosophy of *NectarCam* is also under development. The NectarCAM camera has a modular design and each module consists of 7 PMTs associated with their readout and trigger electronics. Each module consists of a focal plane module, a front-end electronics board, and a back-plane. The front-end board contains the NECTAr chips which perform the readout together with the analog-to-digital conversion and the local trigger electronics [82].

Small-Size Telescopes (SST): Detection at the highest energies from 50 to 300 TeV encounters the problem of the sparseness of the signal from extremely bright γ-ray sources. This leads to the requirement of a few tens of telescopes of small sizes (5-m-diameter class) covering an area of ~ 10 km^2 with very wide FoV (7°–10°), so that air showers can be seen in stereo by widely separated detectors and relatively coarse pixelization (0.25° approximately). Such an array is mainly preferred for the southern observatory where galactic γ-ray sources are our prime targets. The need for a large FoV due to large inter-telescope spacing would actually require a novel solution for these types of telescopes which have been explored. The possibility of the use of a dual-mirror Schwarzchild–Couder optical design with a very small plate scale, thus allowing for a smaller camera with novel technologies like Silicon photomultipliers, is being explored [83].

CTA will become a worldwide project for the future VHE γ-ray astronomy with Cherenkov telescopes. As the first phase of the project, CTA consortium has finalised the "Alpha Configuration" [6], which will consist of 4 LSTs and 9 MSTs in the northern hemisphere and 14 MSTs and 37 SSTs in the southern hemisphere. CTA will not only consolidate VHE γ-ray astronomy as a major branch of astronomy, but will be eventually considered as one of the leading astronomical observatories of the world with tremendous synergies with other facilities in other wavelengths, for example, ALMA (mm wavelength), Thirty Meter Telescope (TMT) in optical, Square Kilometer Array (SKA) in radio, eROSITA in X-rays, and Large Synoptic Survey Telescope (LSST) which are expected to start operations in the next decade.

[5] The first LST constructed at La Palma has an FoV of 4.3°.

[6] https://www.cta-observatory.org/science/ctao-performance/.

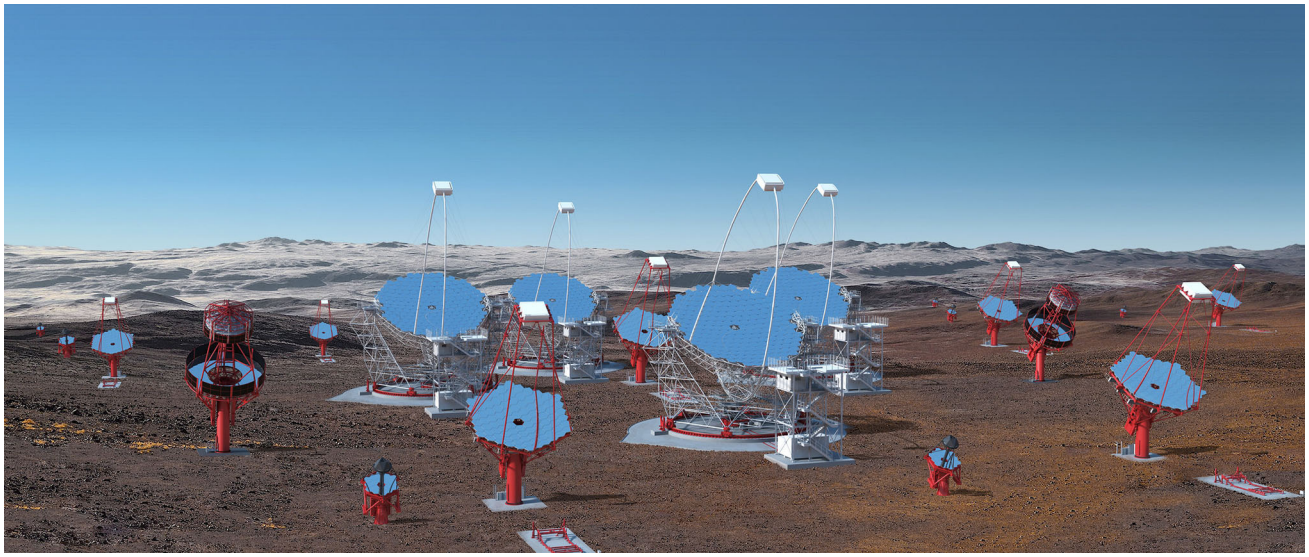

Fig. 13 An artistic illustration of the proposed CTA. Image credit: Gabriel Pérez Diaz, IAC/Marc-AndréBesel, CTAO

Fig. 14 The prototype Large-Size Telescope (LST) installed in La Palma, Canary Island, Spain. Picture credit: Iván Jiménez (IAC), CTAO

6 Simulations and data analysis

Monte Carlo simulations of EAS form an integral part of the atmospheric Cherenkov technique. In the absence of direct calibrations, simulations provide the only way to understand and estimate the performance of the telescope system. Apart from this, simulations provide important inputs for the design of the telescope system and play a major role in data analysis and improvement of sensitivity of the instrument.

Several software packages were developed to simulate EAS initiated by γ-rays as well as various cosmic ray species and also to simulate Cherenkov light production by relativistic charged particles in EAS. Some of the packages used for simulations are MOCCA [84], ALTAI [85], KASCADE [86], and CORSIKA [87,88]. These were used extensively for simulations of previous generation telescope systems. During the last 15 years, CORSIKA has emerged as a package used most extensively for air shower simulations.

CORSIKA (i.e., Cosmic Ray Simulation for KAscade) is a detailed Monte Carlo program which is used to study the evolution of EAS initiated by γ-rays and various particles like protons, nuclei, etc. [87,88] (see CORSIKA website[7]). Originally developed for simulations of the KASCADE experiment at Karlsruhe, COR-

[7] https://www.iap.kit.edu/corsika/.

SIKA has evolved over the last 3 decades since its first version in 1989, and by now, it is used for simulations of various atmospheric Cherenkov ($E \sim 10^{12}$ eV), air shower ($E \sim 10^{20}$ eV), as well as neutrino experiments.

While simulating air showers initiated by various cosmic ray species, CORSIKA deals with interactions between hadrons, nuclei, electrons, photons, etc. It uses a variety of models for low energy and high energy hadronic interactions. For high energy hadronic interactions, one can choose between VENUS, QGSJET, DPMJET based on Gribov–Regge theory, SIBYLL which is mini-jet model, and HDPM which is a phenomenological generator adjusted with experimental data whenever possible, NEXUS and EPOS based on accelerator data. Options available for low energy hadronic interactions include GHEISHA which is a Monte Carlo program, FLUKA which is a refined model with many details of nuclear effects, and UrQMD which describes microscopically the low energetic hadron–nucleus collisions. Furthermore, CORSIKA uses EGS4 code for treating interactions of electrons and photons. In addition to this, simulation of Cherenkov photon production by relativistic particles in EAS is also available as a part of CORSIKA. IACT routines provided by Bernlohr are particularly useful for treating Cherenkov radiation for IACTs [89].

CORSIKA provides an option between various atmospheric profiles such as US standard atmospheric profile parameterised by J. Linsley, profiles for Central Europe, south Pole, tropical region, etc. Atmospheric density variation is modelled in these profiles which is crucial for the evolution of shower and Cherenkov production. Depending on observation location, the appropriate profile can be selected. CORSIKA also takes into account the the deflection of charged particles in the shower by geomagnetic field at the location of the telescope. Wavelength-dependent absorptions of Cherenkov photons such as atmospheric absorption, mirror reflectivity, and the quantum efficiency of PMT are also implemented in the code. Finally, geometry of the telescope array can be given as input parameters.

At the output, CORSIKA gives the distribution of particles, γ-ray photons, and Cherenkov photons reaching the observation level. For each Cherenkov photon hitting telescopes, its location, arrival time, arrival direction, and production height are recorded in the output file.

Figure 15 shows typical simulated cascades for γ-ray and proton primaries. Combining Cherenkov photon distribution with detector specific features such as pulse shape, trigger criteria, NSB at observation site, etc., performance parameters are evaluated. GHS parameters, which play a major role in improving sensitivity for detection of γ-ray signal against cosmic ray background are also obtained from simulations.

Performance parameters indicate various characteristics of the telescope system. These parameters are used in the analysis of the data on celestial objects recorded by telescopes and are also useful for comparing various telescope systems. These parameters, obtained from simulations, are described below.

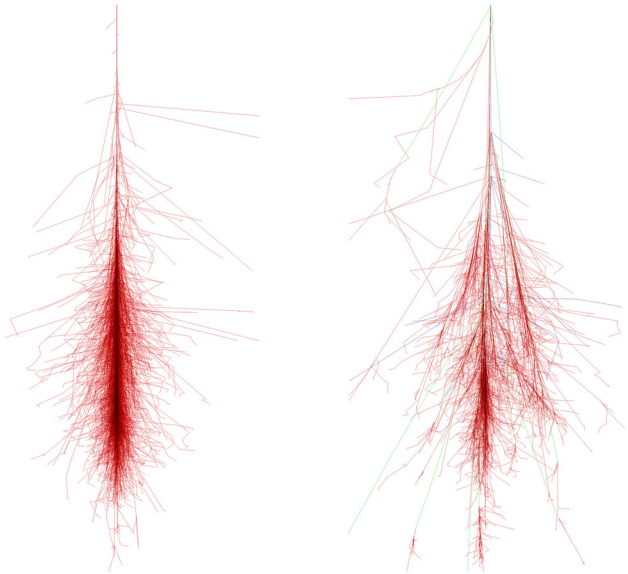

Fig. 15 Left: EAS generated by 100 GeV γ-ray; right : EAS generated by 100 GeV proton primary. Image Credit: CORSIKA website https://www.iap.kit.edu/corsika

The first parameter is energy threshold, i.e., the lowest energy of γ-ray that can be detected by the telescope. It depends on several parameters specific to the telescope system such as the size of the reflector, quantum efficiency of PMTs, NSB at observation site, trigger criteria, observation site altitude, etc. Typically, peak of the differential rate curve generated with simulated γ-ray showers is used as a measure of energy threshold.

The second parameter is the effective collection area, mentioned earlier. This area is much larger than the physical area of the light collector or reflector and is comparable to the size of the Cherenkov pool, which roughly corresponds to a circular area with a radius of about 120 m at observatory locations at moderate altitudes. The effective collection area is energy-dependent, largely decided by the trigger efficiency. It is given by the following equation:

$$A_{\text{eff}}(E) = 2\pi \int_0^\infty R\eta(R, E)\mathrm{d}R, \tag{1}$$

where $\eta(R, E)$ is the trigger probability and R is the distance from shower core.

The next parameter is sensitivity for detection of γ-ray signal in the presence of background produced by cosmic rays. Apart from telescope parameters, it largely depends on the ability to reject cosmic ray background while analysing the data, achieved using various GHS parameters.

The sensitivity of the instrument is defined as the minimum flux from a steady point-like source to be detected in 50 h for 5 standard deviations and is estimated in narrow bins of energy. When the background is perfectly well estimated, the significance of the detection of a source can be computed using a simple formula

$$S = \frac{N_\gamma}{\sqrt{N_{cr}}}, \tag{2}$$

where N_γ and N_{cr} are the excess and background events, respectively. One can thus define the sensitivity S as the flux of the source yielding $N_\gamma/\sqrt{N_{cr}} = 5$ after 50 h of observation. However, the sensitivity is more realistically calculated using Equation 17 of [90] which is a standard method in calculating significances in VHE γ-ray astronomy. To assess the performance of an IACT for sources with any shape, one determines the differential sensitivity calculated in narrow bins of energy (typically 4 or 5 bins per decade). Often, several other conditions like $N_\gamma > 10$ and $N_\gamma > 0.05N_{cr}$ are imposed during the estimation of the sensitivity. The first condition ensures that we are dealing with Gaussian distribution and the second condition ensures that one is not limited by the systematics of background determination which may happen when a small signal resides over a large background.

Simulations play a major role in the analysis of data from wavefront sampling arrays as well as IACTs. Apart from providing performance parameters, they have played an important role in improving the sensitivity of IACTs. In the next few paragraphs, we outline the procedure for the analysis of data from IACTs.

The raw data in the case of an IACT consist of a digitally sampled trace of a signal for each PMT in the camera. In the first step, the pedestal (a baseline value in the absence of any Cherenkov photon) is subtracted during the extraction of the signal. In the next step, those pixels which contain information about Cherenkov photons above a pre-defined threshold are identified. The Cherenkov photons are produced by the EAS trigger pixels, and thus, an image of the shower is formed along with NSB and electronic noise. Hence, the image from the shower needs to be cleaned. The resulting cleaned image is then parameterized based on a moment fitting approach, commonly known as "Hillas parametrization", briefly mentioned in the previous section. It is the most commonly used method given the elliptical nature of the shower images, as shown in Fig. 5. An alternative technique has also been later developed based on semi-analytical method of fitting shower images [91–93]. In the commonly used method of image parameterization, several parameters of the image are calculated (parameters are listed in table 3).

For a single telescope, the shower images are parameterized where parameters of the shower like *length*, *width*, and orientation of the shower are calculated [36]. The cosmic ray showers which produce similar Cherenkov images on the camera plane far outnumber the γ-ray showers. Using the above mentioned parameters, the showers induced by the two primaries can be well discriminated. The power of discrimination improves tremendously when two or more telescopes are deployed and multiple telescopes view the same shower [94] in stereoscopic technique pioneered by HEGRA. The stereoscopic observation allows one to perform a purely geometrical reconstruction of the shower in three dimensions. The images from multiple telescopes can suitably be combined to give very useful information regarding the shower core, shower axis direction, and height of the shower maximum, and hence, the stereo-

Table 3 Several image parameters used for the parameterization of the image on the camera plane. These parameters are later used in the analysis

Parameters	Description of the parameters
Size	Total number of phes in the shower image. Size is proportional (at first approximation) to the energy of γ-ray photon that induced the shower
CoG	Centre of gravity of the image formed at the camera. This parameter determines the position of the weighted mean signal in the camera
Length	Semi-major axis of the elliptical fit to the image. This is related to the longitudinal development of the shower
Width	Semi-minor axis of the elliptical fit to the image. This is related to the lateral development of the shower
Conc-n	Fraction of the phe-s contained in the n brightest pixels
Leakage	Fraction of signal in the outer rings of the image to the total size. only a part of the showers with large impact parameters are captured in the images leading to a wrong estimation in energy. Low leakage value means the image can be properly parameterized and energy determined properly
Alpha	The angle between the major axis and the line joining the CoG with the position of the source in the camera
Dist	The distance between the CoG and the position of the source in the camera
Time gradient	The arrival time of the events in each pixel along the major axis is fitted with a linear function. The linear coefficient is termed as the time gradient
Time RMS	The spread of the arrival times of the pixels in the image

scopic method vastly improves the sensitivity of the telescope system.

Most of the events registered by an IACT are produced by cosmic rays, and hence, γ-ray signal has to be extracted by suitably rejecting all the cosmic ray showers on the basis of information from the image shape and reconstructed direction. Several methods are employed to perform GHS effectively. The simplest of them is to apply cuts judiciously on length and width parameters. This was initially developed by the Whipple group when the observations on putative γ-ray sources were carried out by a single telescope. For stereoscopic observations, the determination of the shower core can be performed from the intersection of the major axes of the images. Once the shower core is reconstructed, the measured widths and lengths of the images can be compared with the width and length parameters generated by Monte Carlo simulations, for images with the same Cherenkov intensity. As a result of this comparison, a quantity called "mean scaled width" and "mean scaled length" can be defined which are used to provide discrimination between γ-ray-induced and cosmic ray-induced showers [94,95]. Another very interesting method was first developed by the CAT collaboration where a model of the shower development based on the knowledge of primary energy, arrival direction, and impact parameter was used. A simple analytical two-dimensional model of shower profile was successfully implemented [91]. This method was further refined to work for multiple telescopes' three-dimensional analytical model of shower development [92]. Other methods like a log-likelihood approach using information from all pixels in the camera [93] and comparisons of template images using Monte Carlo simulations have also been used where it has been shown that the sensitivities obtained from these methods may be better than the simple Hillas parameterization method. More advanced techniques have recently been developed by various groups based on multivariate analysis like Random Forest, Neural Network, etc. [96]. Whatever be the method of discriminating γ-ray and cosmic ray induced showers, most of them have shown very high background rejection efficiency ($> 99\%$) while retaining 75—80% of the γ-rays. Stronger cuts with lower γ-ray efficiencies are also quite often used for discovering a weak source.

The standard mode observation in IACT is the so-called "wobble-mode" [97]. In this method, the telescopes are pointed slightly away from the source position and hence allow the observations of ON- and OFF-regions simultaneously (see Fig. 16). Thus the systematics involved in the determination of the background can be controlled and it also allows for a more effective use of the observation time. The choice of this offset is optimized based on two effects: (1) a too small offset may result in overlap between the ON and OFF region which degrades background estimation, and (2) a too large offset may strongly affect the detection efficiency of the source. Depending on the extension of the source region, multiple OFF-regions can be selected. For a single OFF position, the diametrically opposite position with respect to the camera centre can be selected. Multiple OFF positions help in the estimation of the background more precisely. These positions are selected symmetrically around the source position in such a way that any inhomogeneity in the field of view of the camera is minimized.

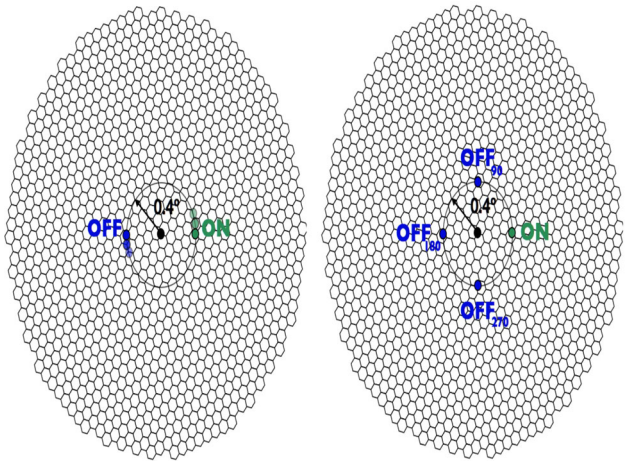

Fig. 16 A typical picture of a wobble-mode observation where the telescope is pointed with a slight offset from the source and the background region [one (**a**) or many (**b**)] can be estimated simultaneously during ON-source observations. This figure is reproduced with permission from Dr. Ruben Lopez Coto's thesis

The reconstruction of the arrival direction of the shower enables one to discriminate between γ-ray photons from the putative source from the abundant isotropic charged cosmic rays. It also helps one to map out the γ-ray emission in case of extended astrophysical sources, especially in our Galaxy which can provide valuable clues to the particle acceleration mechanisms in the source. The angular resolution is energy-dependent and one can attain a very good resolution of better than 0.1° for 68% of the γ-rays from a point source at 1 TeV. At lower energies, the angular resolution tends to degrade owing to the lower number of Cherenkov photons available and due to shower to shower fluctuations.

The event-wise direction reconstruction is estimated using the so-called DISP (Distance between the Image centroid and the Source Position) method, where DISP parameter is defined as the distance between the CoG (Centre of Gravity) and the impact point (see Fig. 17). Using this method, the position of the incident γ-ray direction on the main image axis at the distance from the image centroid is determined. In this case, two positions on each side of the image centroid are possible. Furthermore, the head–tail discrimination is performed using the image parameters that characterize the asymmetry of the image. Typically, the time gradient of the development of the shower along the major axis or the third moment is used to perform this discrimination and hence determine the most probable γ-ray direction.

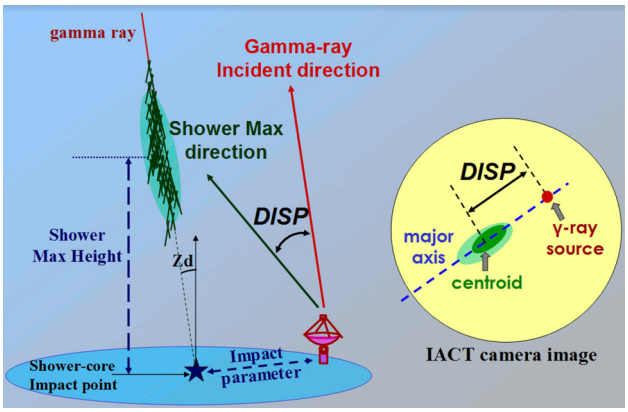

Fig. 17 A schematic diagram of the DISP (distance between the Image centroid and the Source Position) parameter. The main principle of the method is to calculate the DISP parameters and then determine the position of the incident γ-ray direction on the main image axis at the distance DISP from the image centroid. The authors acknowledge the MAGIC collaboration for providing this diagram

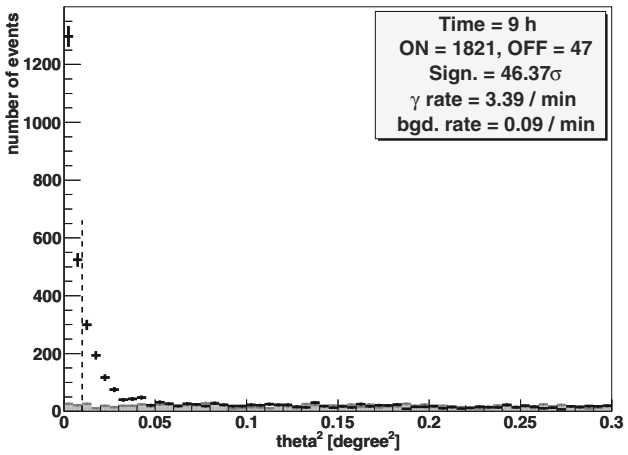

Fig. 18 A typical θ^2 distribution from the direction of the Crab nebula showing the signal events (black) and the background events (grey) above an estimated energy of 300 GeV. The vertical dashed line shows the cut on θ^2 applied to calculate the significance from signal and background region. The figure is reproduced with permission from [98]

The angular resolution is typically defined as the angular distance around the source which contains 68% of the excess γ-ray events. However, in several cases, it is also defined as the standard deviation of a two-dimensional Gaussian fitted to the distribution of reconstructed excess events. Such a 2-D Gaussian corresponds to an exponential fit for the distribution and corresponds to approximately 39% containment of the excess events.

The energy of the event is reconstructed using suitable Look-Up Tables (LUTs), a multi-dimensional table containing mean energy for each combination of the image parameters. The LUTs are created using simulated γ-rays relating the event energy to the impact and Cherenkov photon density measured by each telescope. Corrections due to zenith, azimuth, and large images which are partially contained in the camera are applied. The final estimated energy is computed as the average of the energies reconstructed individually for each telescope, weighted by the inverse of their uncertainties. Typical energy resolutions of current generation IACTs are about 15% at 1 TeV and degrade to around 25% at lower energies ($\sim$ 100 GeV).

To estimate the excess events from a putative source and also calculate its significance, the squared angular distance between the nominal source position in the camera and the reconstructed source position is used. This quantity, called θ^2, is then plotted. The background is estimated by potting the θ^2 distribution in the OFF-regions, as shown in Fig. 18. After suitable normalisation is done in the region where one expects no signal or excess, the number of excess events is then calculated which is the difference between the number of ON events and the number of OFF events. The significance of the excess is calculated using Li and Ma [90].

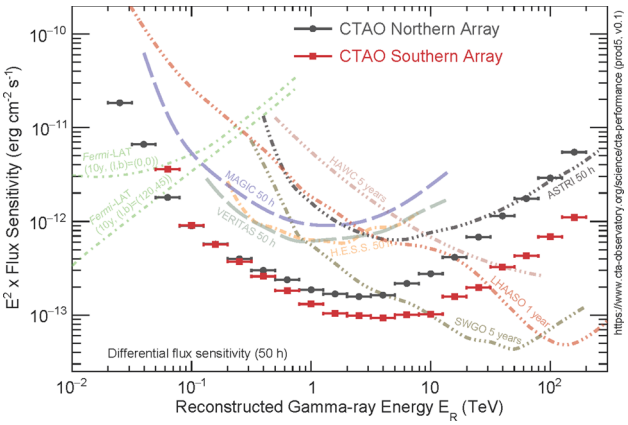

Fig. 19 Differential flux sensitivity of the "Alpha Configuration" of CTA arrays. The sensitivities of the current generation of IACT, high energy γ-ray instruments like Fermi-LAT, and very high energy γ-ray instruments like HAWC are also shown for comparisons. The figure is reproduced with permission from CTA collaboration (https://www.cta-observatory.org/science/ctao-performance/)

To estimate the flux of γ-rays from a source, the knowledge of effective area of the detector is required. The effective area is energy-dependent and is calculated using simulated γ-ray showers over a wide range of impact parameters and an energy distribution close to that of the source (typically a power law at TeV energies).

As has been explained earlier, the sensitivity of a VHE γ-ray instrument is defined as the minimum flux of γ-rays observed from a putative source at a significance of 5σ in a typical observation time of 50 h. Figure 19 shows the differential flux sensitivities (sensitivity in bins of energy) of the "Alpha Configuration" of CTA arrays w.r.t. the present generation of IACTs. Along

with that, we have also plotted the sensitivities of space-based detectors (for e.g., Fermi-LAT) and ground-based air shower array detectors (for e.g., HAWC) for various time scales. Typically, a satellite-based detector has a lower γ-ray collection efficiency owing to the limited size of the detector and hence requires longer integration times to detect an appreciable number of high energy photons. This limits the sensitivity of the space-based detectors at high energies beyond a few GeV. The sensitivities of the air shower array detectors are inferior to the VHE γ-ray detectors (see Fig. 23) owing to the fact that they have worse gamma-hadron separation and poorer angular resolution and hence also require longer observation times (typically about a year or more) to detect a flux comparable to the IACTs. The sensitivities of the IACTs start to worsen at energies around a few tens of GeV owing to the poor gamma-hadron separation at these energies and also at energies beyond a few tens of TeV, because at these energies, the sensitivity is limited by the statistics of the number of photons from the source. The best operating range of the IACTs is from 50 GeV to 50 TeV where most of the important discoveries in the field have been made.

7 Air shower arrays

Apart from the detection of Cherenkov light, there is a complementary way to detect γ-rays on the ground indirectly, by detecting charged secondaries present in the EAS. These secondaries can be detected in two ways: Water Cherenkov Technique (WCT) and Extensive Air Shower (EAS) array technique. In WCT, detectors located inside the water tank or pool detect Cherenkov radiation produced by charged particles present in the shower. For the EAS array technique, charged particles are detected by an array of particle detectors like scintillation detectors spread over a large area. Both these techniques require secondary charged particles at the observation level for a trigger. Therefore, they have a higher energy threshold compared to ACTs and are usually located at very high altitudes. The existence of a large number of muons in hadronic air showers compared to γ-ray showers provides air shower arrays with a tool to distinguish between these two types of primaries. For an EAS initiated by a vertically incident γ-ray with energy 100 TeV, approximately 20,000 shower particles will survive at an altitude of 2 km, and for a 1 TeV γ-ray, there will be a few hundreds of charged particles only. The corresponding numbers at an altitude of 4.5 km would be 100,000 for a 100 TeV γ-ray and a couple of thousands for a 1 TeV γ-ray-induced showers. Even though the energy thresholds of air shower experiments are higher, they have certain advantages over ACTs. These detectors can operate 24×7 and their field of view is 2 sr, i.e., they can observe half of the sky. Angular resolutions of air shower arrays are inferior to ACTs. However, because of large sky coverage and almost 100% duty cycle, they are useful for the detection of transient sources and sky surveys. These arrays are particularly suitable for searching PeVatrons in the Milky Way.

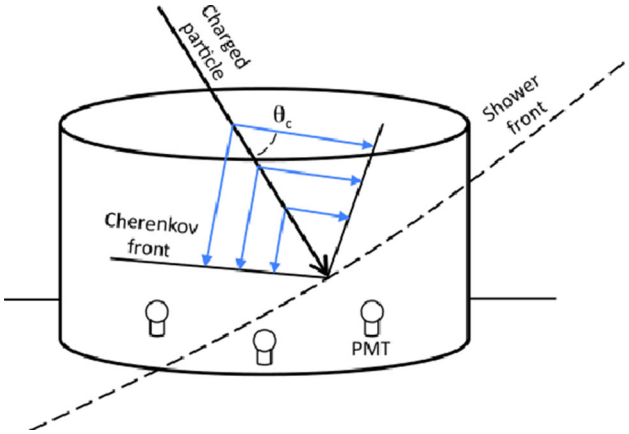

Fig. 20 Water Cherenkov technique: the secondary charged particles present in the EAS will produce Cherenkov photons inside water tanks, which are detected by PMTs located at the bottom of each tank. Image courtesy: HAWC collaboration

7.1 Water Cherenkov Technique

In Water Cherenkov Technique (WCT), an array of PMTs is placed inside a water tank or a pool. These PMTs detect Cherenkov radiation emitted in the water by the secondary charged particles present in EAS (see Fig. 20). In water, the Cherenkov emission angle is large ($\sim 41^\circ$); hence, PMTs can be placed with larger spacings between them. The Multiple Institution Los Alamos Gamma-Ray Observatory (MILAGRO) detector [99,100] built following WCT, consisting of a large water pool of area 60 m $\times$ 80 m and depth of 8 m, was located in New Mexico at an altitude of 2630 m. To prevent contamination from the ambient light, entire pool was covered with a light-tight cover. There were 723 PMTs of 20-cm diameter arranged in two layers, with 450 PMTs in the top layer at a depth of 2.5 m and remaining PMTs at the bottom of the water reservoir. The top layer was used to tag muons. Muon tagging is necessary to discriminate γ-ray showers from cosmic ray showers. The muon content of γ-ray initiated showers is negligible as a cross-section for photo-pion production is very small compared to cross-section for pair-production. On the other hand, hadron-initiated showers have a large number of muons, which survive till the observational level.

Based on the experience gained with MILAGRO, the High-Altitude Water Cherenkov[8] (HAWC) experiment is built, which is located on the Sierra Negra volcano in Mexico at an altitude of 4100 m (see Fig. 21) [101–103]. There are 300 steel tanks, 5.4 m in height and 7.3 m in diameter, filled with purified water, spread over an area of 22000 m^2. Each tank contains a light-tight plastic bladder, which is filled with water to a

[8] https://www.hawc-observatory.org/.

Fig. 21 The High-Altitude Water Cherenkov (HAWC) Experiment. Picture courtesy: HAWC collaboration

depth of 4.5 m, ensuring that particles in the shower are fully absorbed. There are four upward-facing 8-inch PMTs located at the bottom of each tank. Electrons and positrons present in the shower produce Cherenkov photons in the water which are detected by the PMTs. Muons present in the EAS initiated by cosmic rays emit Cherenkov radiation along their path inside the tank before exiting. These muons usually pass closer to one PMT than to the rest, thereby producing an excess signal in one PMT, which can be used to discriminate cosmic ray induced events from γ-ray-induced events. HAWC has carried out the most sensitive sky survey with FoV > 1.5 sr and with a duty cycle of more than 90% at TeV energies till date. It has detected γ-rays above 100 TeV from some galactic sources [104].

7.2 Particle detector arrays

The Extensive Air Shower Arrays use solid-state detectors to detect charged secondaries present in EAS. One such array called Tibet air shower array or Tibet ASγ is located at Yangbajing in Tibet, China at an altitude of 4300 m a.s.l. It is operational since 1990 and went through gradual upgradations over several years. From the configuration of 533 fast timing (FT) plastic scintillators of 0.5 m^2 area each, spread over 22050 m^2 in 1999, it was upgraded to 761 FT scintillator counters and another 28 density (D) counters with effective area of 36900 m^2 in December 2003 [105]. Later, water Cherenkov muon detectors with an area of ~ 3400 m^2 were added to this array by 2014 [106]. This array has an angular resolution of about 0.2° at 100 TeV. γ-ray event selection is based on direction reconstruction and consequent rejection of isotropic cosmic ray background for air shower array with only scintillators. Using this method, signal from Crab nebula was successfully detected at energies above 3 TeV [107]. This was the first clear detection of γ-ray signal from a point source using an air shower array. This was followed by successful detection of blazars Mrk 501 and Mrk 421. After incorporating water Cherenkov muon detectors in the array, based on measured muon numbers in the shower, cosmic ray rejection was improved to 99.92% with energies > 100 TeV leading to the first detection of photons with $E > 100$ TeV from Crab nebula [106].

There is another air shower array located at Yangbajing, Astrophysical Radiation with Ground-based Observatory at YangBaJing (ARGO-YBJ). It consists of a single layer of Resistive Plate Counters (RPCs), operated in streamer mode and with a modular structure. The basic module is a cluster covering an area of 5.7 m $\times$ 7.6 m composed of 12 RPCs, each with an area of 1.23 m $\times$ 2.85 m. There are 130 clusters in the central carpet of 74 m $\times$ 78 m with an active area of $\sim$ 93%. This central carpet is surrounded by 23 additional carpets or guard rings. The total area of the array is 110 m $\times$ 100 m [108,109]. Using arrival time information of shower at various RPCs, the position of shower core and arrival direction of primary is reconstructed. Several sources like Crab, Mrk 421 have been detected at energies above 300 GeV successfully [108].

Based on these previous experiences with ARGO-YBJ, the Large High-Altitude Air Shower Observatory (LHAASO) is being established in China [110–112]. LHAASO is under installation at a high-altitude (4410 m) location at the Daochen site, Sichuan Province. This experiment is designed with multiple detecting methods, to carry out 3D observations of the EAS and is expected to have much better sensitivity in comparison with the previous similar experiments.

The LHAASO experiment mainly includes three detector sub-arrays; 1.3 km^2 array (KM2A), the cen-

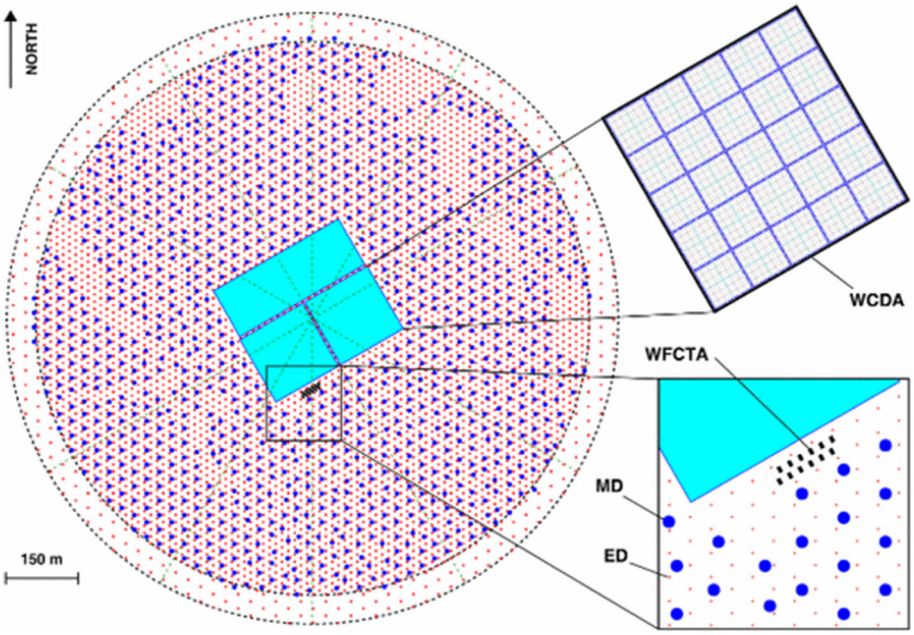

Fig. 22 The layout of the LHAASO observatory. Multiple components of this experiment are shown separately. Image courtesy: LHAASO collaboration

tral part is the Water Cherenkov light Detector Array (WCDA), consists of three ponds with a total area of 78,000 m^2; there is also a telescope array (WFCTA), which is composed of 18 Wide Field Cherenkov light Telescopes (WFCTs) (see Fig. 22). The whole KM2A array consists of 5195 Electromagnetic Detectors (ED), 1 m^2 each and 1188 Muon Detectors (MD), 36 m^2 each. The KM2A can identify γ-ray showers from cosmic ray showers using MDs. At energies around 1 PeV, it has unprecedented rejection power of $\sim 10^{-5}$. KM2A detects γ-rays with energies > 0.1 PeV. The energy resolution and angular resolution of KM2A are <20% and 0.25°, respectively. WCDA can detect low energy (0.1 TeV) γ-rays compared to KM2A. WCDA is ideal to carry out deep surveys for high energy sources. WFCTA detects Cherenkov light emitted by air showers produced by cosmic rays and γ-rays. These telescopes have wide field of view 32° × 112°. The current sensitivity of LHAASO is already an order of magnitude better compared to ACTs in the energy range of 100 TeV and above [113]; see Fig. 23. In its early years of operation, LHAASO has detected several candidate PeVatrons in the galactic plane with high significance [114].

The new hybrid multi-component Tunka Advanced Instrument for cosmic ray physics and Gamma Astronomy (TAIGA) experiment aims to detect air showers induced by γ-rays and cosmic rays. The TAIGA experiment is located at the Tunka valley (altitude 650 m), 50 km West of Lake Baikal, Russia. TAIGA-IACT and TAIGA-HiSCORE will be used to detect VHE γ-rays above 30 TeV (see Fig. 24). TAIGA-IACT [116] will be an array of 16 IACTs. The reflector area of each telescope will be 10 m^2 and the imaging camera will have 560 PMTs. TAIGA-HiSCORE (Hundred Square km Cosmic ORigin Explorer) [117] will be an array of integrating Cherenkov detectors with a wide field of view (0.6 sr). Each detector station will consist of 4 large area PMTs. There will be 100 such detectors (with 150–200-m detector spacing) covering an area of ~ 5 km^2.

All the air shower arrays mentioned above, LHAASO, HAWC, and TAIGA, even with their wide field of view, cannot access sources located in the southern hemisphere, which include the galactic centre. Hence, to achieve full sky coverage, a southern array is under consideration. Southern Wide-field Gamma-ray Observatory (SWGO)[9] is proposed to be built in the Andes at an altitude of 4.4 km a.s.l. [118]. The proposed array will consist of water Cherenkov detectors aided by muon detectors for better gamma-hadron separation.

Another experiment which is primarily devoted to the study of cosmic ray origin, composition, propagation, and anisotropy at energies $> 10^{14}$ eV, but also performs observations in UHE γ-ray Astronomy is the GRAPES-3 (Gamma-Ray Astronomy PeV EnergieS phase-3) experiment located at Ooty, India. This array consists of a combination of plastic scintillators to detect air shower particles along with a large area muon detector. Observations began in the year 2000, with an array consisting of 217 plastic scintillators and a 560 m^2 area muon detector made up of proportional counters. The array was expanded further and currently it is operating with $\sim$ 400 plastic scintillators spread over an area of 25,000 m^2 [119]. Search for γ-rays with energies above 30 TeV from Crab nebula is being attempted with this array [120].

8 Conclusion

Very high energy γ-ray astronomy has undergone a remarkable transformation in the last 3–4 decades. Initially, progress was very slow; first attempts were made

[9] https://www.swgo.org/SWGOWiki/doku.php.

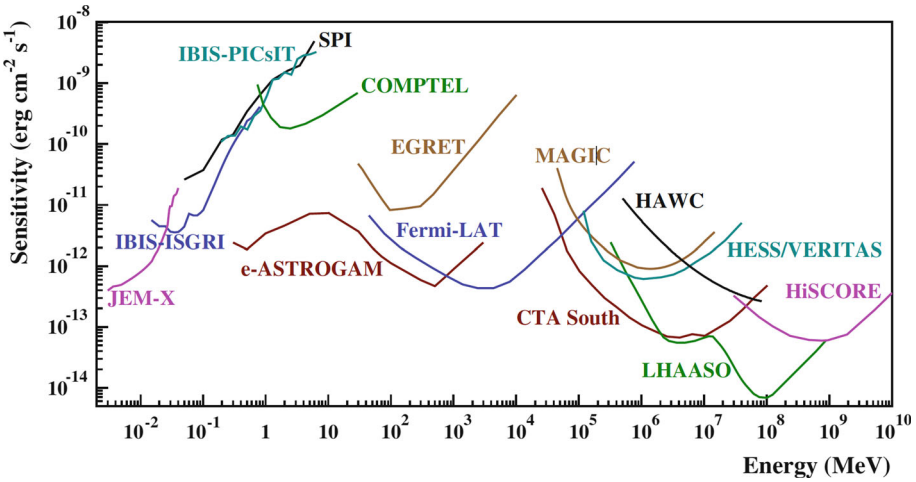

Fig. 23 Point source differential sensitivity curves for different X-ray and γ-ray instruments. For IACTs, e.g., MAGIC, VERITAS, H.E.S.S., and CTA sensitivities are obtained for 50 h. For HAWC, sensitivity is estimated for 5 years and for LHAASO 1 year. Figure is reproduced with permission from [115]

Fig. 24 One of the TAIGA-HiSCORE integrating Cherenkov detector stations with a wide Field of View is seen at the front in the above photograph. Each detector station consists of 4 large area PMTs. One installed TAIGA-IACT telescope seen at the back. Picture courtesy: TAIGA Collaboration

in the 1960s, but astronomers had to wait for almost three decades before the first source was detected in the 1980s by Whipple γ-ray telescope. Whipple telescope proved that the imaging technique is the most powerful method to identify γ-ray initiated showers from overwhelming background of cosmic rays. Following the footsteps of Whipple, the current generation of telescopes, H.E.S.S., MAGIC, and VERITAS have revolutionised VHE γ-ray astronomy. In the beginning of this century, only a handful of sources were detected by ground-based telescopes, and at present, the number of sources detected is more than 200. It is expected that the number of sources detected by the upcoming CTA will be few thousand. On the other hand, Air Shower Array experiments like HAWC and LHAASO will carry out extensive surveys at Ultra High Energy regime and with higher sensitivities above 100 TeV. Ground-based γ-ray astronomy is now entering a fascinating phase and is going to play a very important role in multi-messenger astronomy in the coming decades.

Acknowledgements DB acknowledges Science and Engineering Research Board—Department of Science and Technology for Ramanujan Fellowship—SB/S2/ RJN-038/2017. PM acknowledges the generous support of the Stanislaw Ulam fellowship (PPN/ULM/2019/1/00096/A/00001) by Polish National Agency for Academic Exchange (NAWA). VRC acknowledges the support of the Department of Atomic Energy, Government of India, under Project Identification No. RTI4002. We thank the editor and referee for their useful comments which improved the manuscript.

References

1. W.B. Atwood et al., Astrophys. J. **697**, 1071 (2009)
2. IceCube Collaboration, Astropart. Phys. **26**, 155 (2006)
3. KM3Net Collaboration, J. Phys. G **43**, 084001 (2016)
4. K. Abe et al., arXiv:1805.04163 (2018)

5. G. Cocconi, Proc. 6th Int. Cosmic Ray Conf. (Moscow), vol. 2, p. 309 (1960)
6. G.T. Zatsepin, A.E. Chudakov, J. Exp. Theor. Phys. **41**, 655 (1961)
7. W. Galbraith, J.V. Jelley, Nature **171**, 349 (1953)
8. P.M.S. Blackett, Physical Society of London Gassiot Committee Report (1948)
9. A.E. Chudakov, V.L. Dadykin, V.I. Zatsepin, N.M. Nesterova, Proc. Lebedev Phys. Inst. **26**, 118 (1964)
10. A.S. Lidvansky, Radiat. Phys. Chem. **75**, 891 (2006)
11. J.V. Jelley, N.A. Porter, Quart. J. Roy. Astron. Soc. **4**, 275 (1963)
12. G.G. Fazio et al., Can. J. Phys. Suppl. **46**, 451 (1968)
13. T.C. Weekes, Nucl. Phys. B, Proc. Suppl. **10**, 41 (1989)
14. A. Hewsish, J.S. Bell, J.D.H. Pilkington, P.F. Scott, R.A. Collins, Nature **217**, 709 (1968)
15. T.C. Weekes, Written version of lectures given at the international heraeus summer school on "Physics with Cosmic Accelerators", Bad Honnef, Germany, July 5–16, 2004. arxiv:astro-ph/0508253 (2005)
16. D. Hill, N. Porter, Nature **191**, 690 (1961)
17. N.A. Porter, Proc. of Intl. Workshop on Very High Energy γ-ray Astronomy, Ootacamund, (Eds: P.V. Ramanamurthy and T.C. Weekes, 1982), p. 64
18. M. de Naurois, D. Mazin, C. R. Physique **16**, 610 (2015)
19. A. Bonardi et al., Exp. Astron. **38**, 1–9 (2014)
20. C.R. Benn, S.L. Ellison, New Astron. Rev. **42**, 503–507 (1998)
21. D. Bose et al., Astrophys. Space Sci. **309**, 111 (2007)
22. P. Baillon et al., Astropart. Phys. **1**, 341 (1993)
23. V. Basiuk et al., AIP Conf. Proc. **220**, 65 (1991)
24. D.M. Gingrich et al., IEEE Trans. Nucl. Sci. **52**, 2977 (2005)
25. E. Pare et al., Nucl. Instr. Methods Phys. Res. A **490**, 71 (2002)
26. F. Arqueros et al., Astropart. Phys. **17**, 293 (2002)
27. D. Hanna et al., Astrobiology **9**, 345 (2009)
28. M. De Naurois, Astrophys. J. **566**, 343 (2002)
29. P. Bruel, Frascati Phys. Ser. **37**, 367 (2004)
30. D.A. Smith et al., Astron. Astrophys. **459**, 453 (2006)
31. S. Oser et al., Astrophys. J. **547**, 949 (2001)
32. L.M. Boone et al., Astrophys. J. **579**, L5 (2002)
33. L. Saha et al., Astropart. Phys. **42**, 33 (2013)
34. J. Kildea et al., Astropart. Phys. **28**, 182 (2007)
35. T.C. Weekes, K.E. Turver, Recent advances in γ-ray astronomy. Ed. by R. D. Wills and B. Battrick, ESA Special Publication, vol. 124
36. A.M. Hillas, Proc. ICRC **3**, 445 (1985)
37. T.C. Weekes et al., Astrophys. J. **342**, 379 (1989)
38. M. Punch et al., Nature **358**, 477 (1992)
39. J. Quinn et al., Astrophys. J. **487**, L5 (1997)
40. M. Catanese et al., Astrophys. J. **501**, 616 (1998)
41. D. Petry et al., Astrophys. J. **580**, 104 (2002)
42. A. Barrau et al., Nucl. Instr. Methods Phys. Res. A **416**, 278 (1998)
43. G. Puhlhofer et al., Astropart. Phys. **20**, 267 (2003)
44. A. Konopelko et al., Astropart. Phys. **4**, 199–215 (1996)
45. F. Aharonian et al., Astron. Astrophys. **370**, 112–120 (2001)
46. F. Aharonian et al., Astron. Astrophys. **439**, 635–643 (2005)
47. F. Aharonian et al., Astron. Astrophys. **403**, L1–L5 (2003)
48. O.R. Kalekin et al., Astron. Lett. **21**, 184 (1995)
49. S. Aiso et al., Proc. 25 th Int. Cosmic-Ray Conf. (Durban), vol. 5, p. 373 (1997)
50. P. Armstrong et al., Exp. Astron. **9**, 51–80 (1999)
51. T. Hara et al., Nucl. Instr. Methods Phys. Res. A **332**, 300–309 (1993)
52. V.G. Sinitsyna et al., Proceedings of ICRC, p. 2798 (2001)
53. F. Aharonian et al., Astron. Astrophys. **457**, 899–915 (2006)
54. H. Abdalla et al., Astron. Astrophys. **612**, A1 (2018)
55. F. Aharonian et al., Phys. Rev. Lett. **101**, 261104 (2008)
56. H. Abdalla et al., Astron. Astrophys. **620**, A66 (2018)
57. J. Aleksic et al., Astropart. Phys. **72**, 61–75 (2016)
58. J. Aleksic et al., Astropart. Phys. **72**, 76–94 (2016)
59. E. Aliu et al., Science **322**, 1221 (2008)
60. S. Ansoldi et al., Astron. Astrophys. **585**, A133 (2016)
61. V. Acciari et al., Nature **575**, 455 (2019)
62. The IceCube Collaboration, Fermi-LAT Collaboration et al., Science **361**, 1378 (2018)
63. M. Ahnen et al., Astrophys. J. Lett. **815**, L23 (2015)
64. M. Ahnen et al., Astron. Astrophys. **595**, A98 (2016)
65. V. Acciari et al., Astron. Astrophys. **635**, A158 (2020)
66. E. Aliu et al., Astrophys. J. **770**, 93 (2013)
67. E. Aliu et al., Astrophys. J. **764**, 38 (2013)
68. E. Aliu et al., Astrophys. J. **788**, 78 (2013)
69. V.A. Acciari et al., Nature **462**, 770–772 (2009)
70. E. Aliu et al., Astrophys. J. **750**, 94 (2012)
71. E. Aliu et al., Astrophys. J. **755**, 118 (2012)
72. A. Abeysekara et al., Astrophys. J. Lett. **815**, L22 (2015)
73. E. Aliu et al., Science **334**, 69 (2011)
74. R. Enomoto et al., Astrophys. J. **638**, 397 (2006)
75. R. Koul et al., Nucl. Instr. Methods Phys. Res. A **578**, 548 (2007)
76. C. Borwankar et al., Astropart. Phys. **84**, 97 (2016)
77. H. Anderhub et al., J. Instrum. **8**, P06008 (2013)
78. B.S. Acharya et al., Astropart. Phys. **43**, 3 (2013)
79. Science with CTA, by CTA Consortium, World Scientific Press (2019)
80. J. Cortina (for the LST collaboration), Proceedings of 36th ICRC, p. 653 (2019)
81. G. Pühlhofer at al., Proceedings of 34th ICRC (2015). arXiv:1509.02434
82. T. Tavernier at al., Proceedings of 36th ICRC, p. 805 (2019)
83. A. Asano et al., Nucl. Instr. Methods Phys. Res. A **912**, 177–181 (2018)
84. A.M. Hillas, Nucl. Phys. B Proc. Suppl. **52**, 29 (1997)
85. A.K. Konopelko, A.V. Plyasheshnikov, Nucl. Instr. Methods Phys. Res. A **405**, 419 (2000)
86. M.P. Kertzman, G.H. Sembroski, Nucl. Instr. Methods Phys. Res. A **343**, 629 (1994)
87. D. Heck, J. Knapp, J.N. Capdevielle, G. Schatz, T. Thouw, Forschungszentrum Karlsruhe Report FZKA 6019 (1998)
88. D. Heck, T. Pierog, Extensive air shower simulation with CORSIKA: a user's guide (Version 7.7402 from December 18, 2020). https://web.ikp.kit.edu/corsika/usersguide/usersguide.pdf

89. K. Bernlohr, Astropart. Phys. **30**, 149 (2008)
90. T.-P. Li, Y.-Q. Ma, Astrophys. J. **272**, 317 (1983)
91. S. Le Bohec et al., Nucl. Instr. Methods Phys. Res. A **416**, 425–437 (1998)
92. M. Lemoine-Goumard, B. Degrange, M. Tluczykont, Astropart. Phys. **25**, 195–211 (2006)
93. M. de Naurois, L. Rolland, Astropart. Phys. **32**, 231–252 (2009)
94. A. Daum et al., Astropart. Phys. **8**, 1–11 (1997)
95. A. Konopelko et al., Astropart. Phys. **10**, 275–289 (1999)
96. J. Albert et al., Nucl. Instr. Methods Phys. Res. A **588**, 424 (2008)
97. V.P. Fomin et al., Astropart. Phys. **2**, 137–150 (1994)
98. J. Aleksic et al., Astropart. Phys. **35**, 435–448 (2012)
99. A.J. Smith for MILAGRO Collaboration, 29th ICRC, vol. 10, pp. 227–242 (2005)
100. R. Atkins et al., Astrophys. J. **595**, 803 (2003)
101. A.U. Abeysekara et al., Astropart. Phys. **35**, 641–650 (2012)
102. A.U. Abeysekara et al., Astropart. Phys. **50–52**, 26–32 (2013)
103. A.U. Abeysekara et al., Phys. Rev. D **90**, 122002 (2014)
104. A.U. Abeysekara et al., Phys. Rev. Lett. **124**, 021102 (2020)
105. M. Amenomori et al., Astrophys. J. **813**, 98 (2015)
106. M. Amenomori et al., Phys. Rev. Lett. **123**, 051101 (2019)
107. M. Amenomori et al., Astrophys. J. Lett. **525**, L93 (1999)
108. G. Aielli et al., Astrophys. J. Lett. **714**, L208 (2010)
109. G. Aielli et al., Nucl. Instr. Methods Phys. Res. A **562**, 92 (2006)
110. G. Di Sciascio for LHAASO Collaboration, Nucl. Part. Phys. Proc. **279–281**, 166-173 (2016)
111. X. Bai et al. arXiv:1905.02773 (2019)
112. F. Aharonian et al., Chin. Phys. C **45**, 025002 (2021)
113. G. Di Sciascio (on behalf of the LHAASO Collaboration), Nucl. Phys. B Proc. Suppl. **00**, 1–8 (2019)
114. Zhen Cao et al., Nature **594**, 33–36 (2021)
115. A. De Angelis, M. Mallamaci, Eur. Phys. J. Plus **133**, 324 (2018)
116. D. Zhurov et al., Phys. Conf. Ser. **1181**, 012045 (2019)
117. O. Gress et al., Nucl. Instr. Methods Phys. Res. A **845**, 367–372 (2017)
118. Ulisses Barres de Almeid, on behalf of the SWGO Collaboration. arXiv:2012.13740 (2016)
119. S.K. Gupta et al., Nucl. Instrum. Methods A **540**, 311 (2005)
120. D. Pattanaik et al., Proceedings of Science PoS (ICRC2021), p. 870